EVALUATION OF METABOLITE VARIATION BETWEEN ACUTE LYMPHOBLASTIC LEUKEMIA (ALL) AND CHRONIC MYELOID LEUKEMIA (CML) CELL LINES VIA TRIPLE QUADRUPOLE LC-MS

A THESIS SUBMITTED TO
THE GRADUATE SCHOOL OF NATURAL AND APPLIED SCIENCES
OF
MIDDLE EAST TECHNICAL UNIVERSITY

BY

CEREN PEKŞEN

IN PARTIAL FULFILLMENT OF THE REQUIREMENTS
FOR
THE DEGREE OF MASTER OF SCIENCE
IN
BIOTECHNOLOGY

OCTOBER 2019

Approval of the thesis:

EVALUATION OF METABOLITE VARIATION BETWEEN ACUTE LYMPHOBLASTIC LEUKEMIA (ALL) AND CHRONIC MYELOID LEUKEMIA (CML) CELL LINES VIA TRIPLE QUADRUPOLE LC-MS

submitted by **CEREN PEKŞEN** in partial fulfillment of the requirements for the degree of **Master of Science in Biotechnology Department, Middle East Technical University** by,

Prof. Dr. Halil Kalıpçılar
Dean, Graduate School of **Natural and Applied Sciences** _____

Assoc. Prof. Dr. Can Özen
Head of Department, **Biotechnology** _____

Assoc. Prof. Dr. Can Özen
Supervisor, **Biotechnology, METU** _____

Assoc. Prof. Dr. Salih Özçubukçu
Co-supervisor, **Chemistry, METU** _____

Examining Committee Members:

Assoc. Prof. Dr. Çağdaş Devrim Son
Biology, METU _____

Assoc. Prof. Dr. Can Özen
Biotechnology, METU _____

Assoc. Prof. Dr. Salih Özçubukçu
Chemistry, METU _____

Prof. Dr. Ece Konaç
Medical Biology, Gazi University _____

Assist. Prof. Dr. Harun Koku
Chemistry Engineering, METU _____

Date:

I hereby declare that all information in this document has been obtained and presented in accordance with academic rules and ethical conduct. I also declare that, as required by these rules and conduct, I have fully cited and referenced all material and results that are not original to this work.

Name, Surname: Ceren Pekşen

Signature :

ABSTRACT

EVALUATION OF METABOLITE VARIATION BETWEEN ACUTE LYMPHOBLASTIC LEUKEMIA (ALL) AND CHRONIC MYELOID LEUKEMIA (CML) CELL LINES VIA TRIPLE QUADRUPOLE LC-MS

Pekşen, Ceren
M.S., Department of Biotechnology
Supervisor: Assoc. Prof. Dr. Can Özen
Co-Supervisor : Assoc. Prof. Dr. Salih Özçubukçu

October 2019, 75 pages

Hematologic cancers have two origins: myeloid and lymphoid. While lymphatic leukemia, originate from the lymphoid cell line, acute myeloid leukemia (AML) and chronic myeloid leukemia (CML) originate from the myeloid cell line.

CML is granulocyte cancer and in this disease, as well as granulocytes, the number of cells that cause blood clotting, which are called platelets, may increase in the blood. In CML, a non-hereditary genetic abnormality, Philadelphia chromosome, where a structural change occurs in chromosome 22, is seen in blood cells. Acute lymphoblastic leukemia (ALL), on the other hand, is caused by abnormally uncontrolled and excessive proliferation of lymphoblasts. ALL is responsible for 80% of childhood leukemia and is common between 3-7 years of age. It can also be seen in adults and accounts for 20% of all adult leukemia. Interestingly, it was recorded that CML in its blast phase can turn into acute leukemia. It is not known which mutations cause this conversion.

Since all leukemia subtypes stem from the bone marrow, the gold standard for the

diagnosis of leukemia types is genetic testing via invasive bone marrow biopsy, but it has a healing process and can have psychological impacts, especially on children, thus recently, metabolomics, non-invasive and fast methods that can help in early diagnosis are being studied in leukemia. The cells obtained via bone marrow biopsy are examined for chromosomal abnormalities with cytogenetics analysis.

In this study, the metabolic differences of Jurkat (ALL) and K562 (CML-BP) cell lines were aimed to be evaluated using HPLC-MS. Quantitative and quasi-quantitative studies were held to have an idea on the amounts of metabolites in each cell line. After measuring the concentrations of lactic acid and citric acid with the use of their authentic standards, a mass screening was performed on both cell lines, and it was seen that the metabolisms that are mainly affected during the conversion are tyrosine, arginine and proline, and glutathione metabolisms. Thus, existence of indicator metabolites of these related pathways were scanned. Intensities of the confirmed metabolites were compared.

This study is the first metabolomics study that focuses on the blastic transformation of CML to ALL. Results of this study can be used in further studies to define a differentiating pattern for CML and ALL.

Keywords: Chronic Myeloid Leukemia, Acute Lymphoblastic Leukemia, Metabolomics, LC-MS, Oncometabolites

ÖZ

AKUT LENFOBLASTİK LÖSEMİ (ALL) VE KRONİK MİYELOİD LÖSEMİ (KML) HÜCRE HATLARI ARASINDAKİ METABOLİT VARYASYONUN TRİPLE KUADRUPOL LC-MS İLE DEĞERLENDİRİLMESİ

Pekşen, Ceren
Yüksek Lisans, Biyoteknoloji EABD
Tez Yöneticisi: Doç. Dr. Can Özen
Ortak Tez Yöneticisi : Doç. Dr. Salih Özçubukçu

Ekim 2019 , 75 sayfa

Hematolojik kanserlerin iki kökeni vardır: miyeloid ve lenfoid. Lenfatik lösemi, lenfoid hücre hattından, akut miyeloid lösemi (AML) ve kronik miyeloid lösemi (KML) ise miyeloid hücre hattından kaynaklanır.

KML, granülosit kanseridir ve bu hastalıkta, granülositlerin yanı sıra, trombosit olarak adlandırdığımız kanın pıhtılaşmasına neden olan hücre sayısı kanda artabilir. KML'de, hastalığın önemli bir belirteci olarak kabul gören, kan hücrelerinde kromozom 22'de yapısal bir değişikliğin meydana geldiği, genetik bir anormallik olan "Philadelphia kromozomu" görülmektedir. Akut lenfoblastik lösemi (ALL) ise anormal kontrolsüz ve aşırı lenfoblast proliferasyonundan kaynaklanır. ALL, çocukluk lösemisinin %80'inden sorumludur ve 3-7 yaş aralığındaki çocuklarda sık rastlanır. Yetişkinlerde de görülebilir ve tüm yetişkin lösemilerinin %20'sini oluşturur. İlginç bir şekilde, blast fazına (BF) ulaşmış KML'nin akut lösemiye dönüşebileceği kaydedilmiştir. Hangi mutasyonların bu dönüşüme neden olduğu bilinmemektedir.

Tüm lösemi alt tipleri kemik iliğinden kaynaklandığı için, lösemi tiplerinin teşhisinde "altın standart" invaziv kemik iliği biyopsisi ile genetik testlerdir, ancak iyileşme süreci vardır ve özellikle çocuklar üzerinde psikolojik etkileri olabilir. Son zamanlarda lösemide erken teşhiste yardımcı olabilecek non-invaziv ve hızlı yöntemler araştırılmaktadır. Kemik iliği biyopsisi ile elde edilen hücreler, sitogenetik analiz ile kromozomal anormallikler açısından da incelenmektedir.

Bu çalışmada Jurkat (ALL) ve K562 (BF-KML) hücre hatlarının metabolik farklılıkları HPLC-MS aracılığıyla değerlendirildi. Her bir hücre hattındaki metabolitlerin miktarı hakkında fikir edinmek için kantitatif ve yarı-kantitatif çalışmalar yapıldı. Otantik standartların kullanımıyla laktik asit ve sitrik asit konsantrasyonları ölçüldükten sonra, her iki hücre hattında da toplu taramalar yapıldı, ve dönüşüm sırasında esas olarak etkilenen metabolizmaların tirozin, arginin ve prolin, ve glutatyon metabolizmaları olduğu görüldü. Ardından, örneklerde bu ilgili yolakları indike eden metabolitlerinin varlığı tarandı. Doğrulanan metabolitlerin konsantrasyonları karşılaştırıldı.

Bu çalışma, KML'nin ALL'ye blastik transformasyonu üzerine odaklanan ilk metabolomik çalışmadır. Bu çalışmanın sonuçları, daha sonraki çalışmalarda CML ve ALL'yi ayırt eden paternler tanımlamak için kullanılabilir.

Anahtar Kelimeler: Kronik Miyeloid Lösemi, Akut Lenfoblastik Lösemi, Metabolomik, LC-MS, Kanser Metabolitleri

To my mother

ACKNOWLEDGMENTS

First, I would like to express my gratitude to my supervisor Assoc. Prof. Dr. Can Özen for his continuous academic support of my MSc study and research, for his motivation and immense knowledge. His guidance helped me during my research and writing of this thesis.

I would like to acknowledge Assoc. Prof. Dr. Naşit İğci for his suggestions and comments.

I grateful to my lab mates Tarık Dinç and Selin Gerekçi for their significant contributions, stimulating conversions, and Hazal Hepşen Hüsnügil, Ezgi Güleç, and Mustafa Nakip for their help.

I cannot thank enough for my friends for encouraging me, supporting me, and trying to cheer me up all the time.

But mostly, I would like to thank my mother Nazan Şenman for her unconditional support, patience, for being the best mother and father ever, and for putting up with all of the obstacles on the way.

TABLE OF CONTENTS

LIST OF TABLES

TABLES

LIST OF FIGURES

FIGURES

LIST OF ABBREVIATIONS

ALL	Acute Lymphocytic Leukemia
AMBIC	Ammonium Bicarbonate
AML	Acute Myeloid Leukemia
BM	Bone Marrow
BPC	Base Peak Chromatogram
CE-MS	Capillary Electrophoresis - Mass Spectrometry
CLL	Chronic Lymphocytic Leukemia
CML	Chronic Myeloid Leukemia
CML-BP	Chronic Myeloid Leukemia in Blast Phase
EIC	Extracted Ion Chromatogram
ESI	Electrospray Ionisation
GC-MS	Gas Chromatography - Mass Spectrometry
LC-MS	Liquid Chromatography - Mass Spectrometry
MSEA	Metabolite Set Enrichment Analysis
MS/MS	Tandem Mass Spectrometry
NAAA	Non-Essential Amino Acid
NMR	Nuclear Magnetic Resonance
TIC	Total Ion Chromatogram

CHAPTER 1

INTRODUCTION

1.1 Hematological Malignancies

Hematopoiesis is the process of blood cell formation and specialization. All types of blood cells are formed in the bone marrow by pluripotent hematopoietic stem cells. During the hematopoiesis process, hematopoietic stem cells (HSC) turn into mature cells through numerous developmental processes, and each mature cell has a specific task. (Figure 1.1)

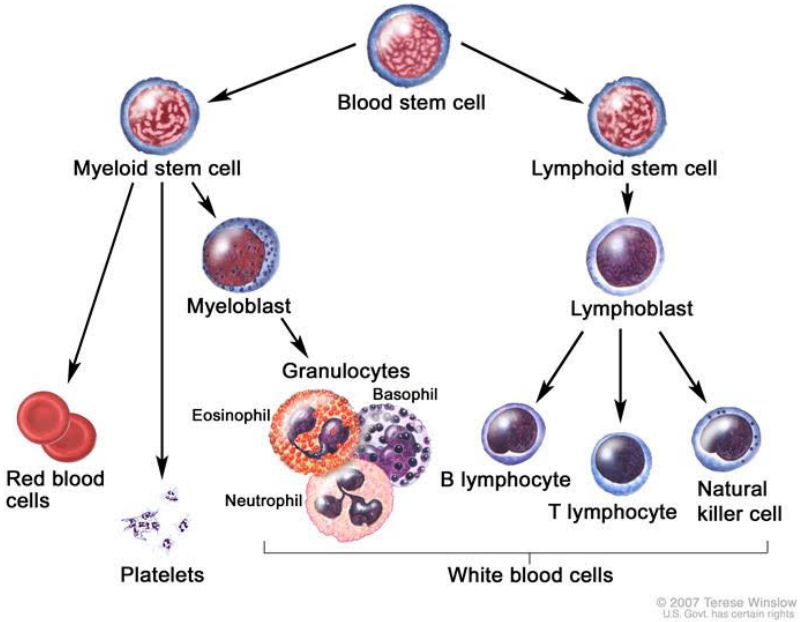

Figure 1.1: Scheme of Hematopoiesis [1]

Hematopoietic malignancies, such as leukemia, lymphoma, and multiple myeloma

are mainly originated from the defects in the genetic structure of immature blood cells. The cell growth arrests and the cells cannot mature further, yet continues to divide. Practically every failure in the hematopoietic process leads to the development of a different type of malignancy.

These cancers have two sources as myeloid and lymphoid. Under normal conditions, myeloid cells evolve into granulocytes, erythrocytes, macrophages, platelets, and mast cells, while the lymphoid cells form NK, B, T, and plasma cells. (Figure 1.2) Whereas in case of a genetic defect, myeloid cells evolve in malignant cells that cause acute and chronic myeloid leukemia, myeloproliferative diseases and myelodysplastic syndromes, and lymphoid cells lead to lymphoma, lymphatic leukemia, and myeloma. [2]

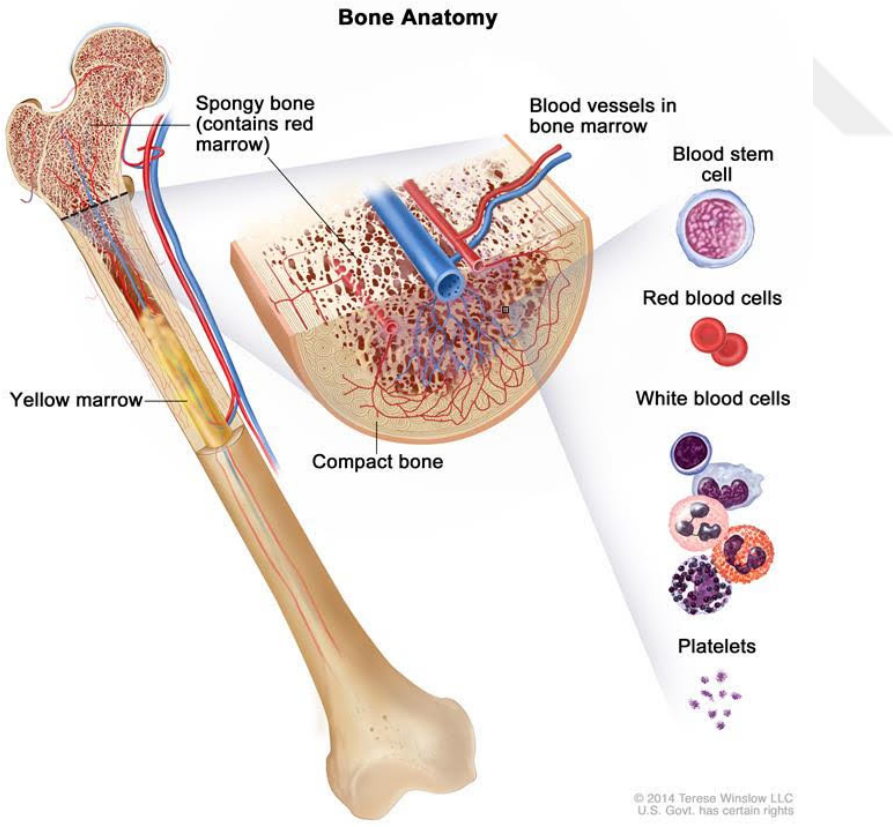

Figure 1.2: Anatomy of BM Tissue [1]

1.2 Leukemia

The word leukemia was acquired from the combination of two Greek words, leukos (white) and haima (blood), and it was used to define a type of malignancy, that reveals itself by abnormal proliferation of blood cells, primarily white blood cells.[3]

Leukemia is traditionally classified according to its morphological characteristics, of which result may diversify according to the researcher. In recent years, cytochemical analyses, immunophenotyping, and enzyme abnormalities techniques are being adopted for the classification and subtyping of leukemia cells.[4]

1.2.1 Leukemia Subtypes

Leukemia cells may comprise mature cells such as in chronic lymphocytic leukemia (CLL), or precursor cells of various strains such as in acute leukemias, or both precursor and mature cells as in chronic myeloid leukemia (CML). Leukemias can occur from any age to newborns to older ones, but different forms have very different age distributions. Acute myeloid leukemia in children is less common than acute lymphoblastic leukemia, which is most common in early childhood and rarely seen in adults. CML is very rare in young children, and CLL, the most common form of leukemia in the Western world, is specific to people over the age of about 40, with an average age of over 70.

1.2.1.1 Chronic Myeloid Leukemia (CML)

CML is granulocyte cancer, and in this disease, as well as granulocytes, the number of cells that cause blood clotting, which we call platelets, may increase in the blood. CML can occur at any age, but most commonly occurs between the ages of 40 and 50, and is very rare in children. Of every 100 leukemia patients, 20 to 30 are CML, which is slightly more common in men than in women.

CML is characterized by a mutant chromosome 22, caused by a translocation between chromosomes 9 and 22, known as the Philadelphia chromosome, resulting in

the genetic combination of the BCR and ABL genes, resulting in the expression of Bcr-Abl kinase. Bcr-Abl is a tyrosine kinase which activates signaling of the MAPK, JAK/STAT, MYC, RAS, and PI3K pathways. Furthermore, Bcr-Abl improves the frequency of cell growth and interferes with the activation of the cell cycle and control pathways, especially those engaged in DNA repair, enabling rapid development and mutation occurrence.

Since the Philadelphia Chromosome cause expression of Bcr-Abl protein, which gives a signal that continuously activates tyrosine kinases which trigger related downstream signalling pathways in the cell, Tyrosine kinase inhibitors (TKIs) are mainly used for the therapy of CML, eg. Imatinib. But TKIs may results in the quick formation of resistant clones, most usually due to point mutations in the kinase domain of BCR-ABL, leading a relapse.

The disease has three stages, which are chronic, accelerated and blastic stage. When patients are diagnosed, they are usually in the stage, as known as the chronic stage. (Figure 1.3) At this stage, the disease is slow and the patients have few complaints, continue their routine lives and are rarely hospitalized. In order to regulate drug doses during this period, they should have regular blood tests and examinations in accordance with the outpatient follow-up. Although the duration of the chronic phase varies from patient to patient, it is 3 to 4 years when not treated or no response is obtained. At the end of this period, patients enter the stage known as the accelerated stage.

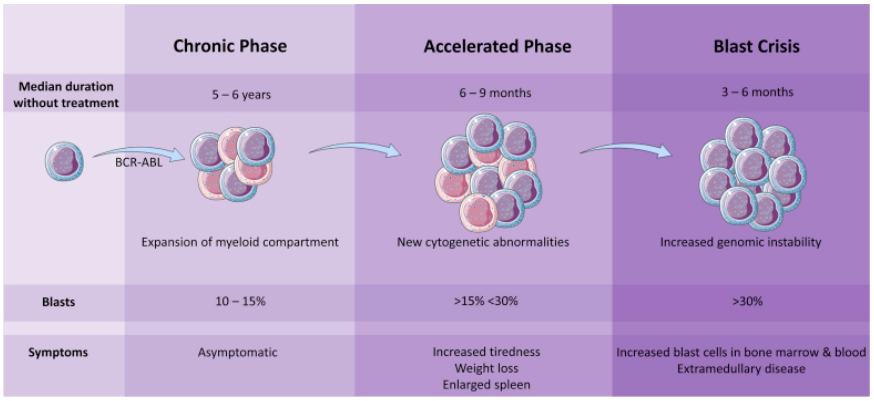

Figure 1.3: Stages of Chronic Myeloid Leukemia [5]

In the accelerated stage, besides the increase in the patient's symptoms (fever, weight loss, fatigue, bone pain, etc.), the spleen size increases during the examinations. The number of blood leukocytes tends to increase further, and the dose of drugs administered to keep this increase in control increases. This period can last from a few months to a year.

After the accelerated phase, the blastic phase develops. At this stage, CML is similar to acute leukemia. During this period, patients develop fever, bruises on the skin, weakness, fatigue, bone pain and so on. During the blastic phase, patients should be hospitalized. The response rate of the blastic phase to treatment is generally low.[6]

1.2.1.2 Acute Lymphoblastic Leukemia (ALL)

ALL is caused by abnormally uncontrolled and excessive proliferation of lymphoblasts. Lymphoblasts proliferate in the bone marrow and then pass into the blood and other organs such as the cerebrospinal cord. ALL is responsible for 80% of childhood leukemia and is common between 3-7 years of age. It can also be seen in adults and accounts for 20% of all adult leukemia. [7]

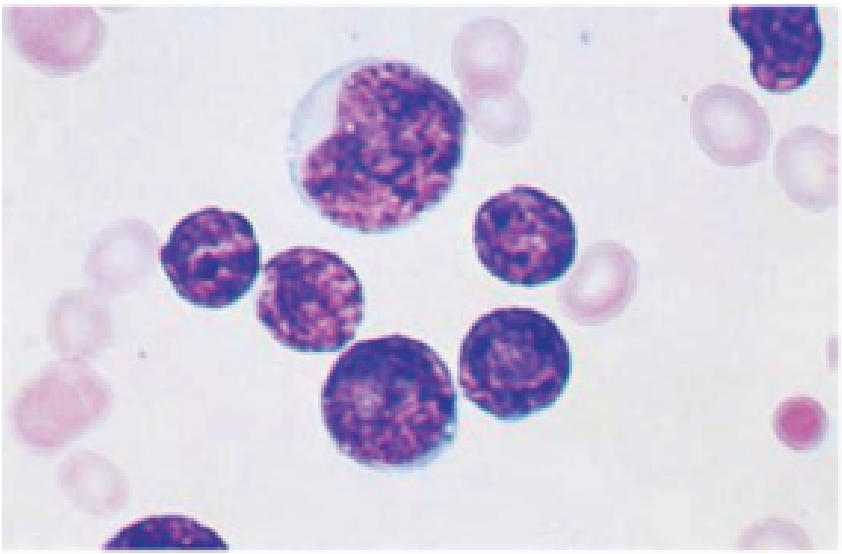

Figure 1.4: ALL Microscopy Image [1]

In ALL, lymphoblasts lose their maturation and differentiation functions. (Figure

1.4) As these cells proliferate rapidly and replace normal cells, the production of erythrocytes, platelets, and leukocytes in the bone marrow is disrupted. [7]

As increased lymphoblasts inhibit the production of blood in the bone marrow, anemia and consequently fatigue, increased breathlessness and pallor occur. Increased lymphoblasts disrupt the production of cells in the immune system, so high fever, tonsillitis and pneumonia may occur. Lymphoblasts accumulate in the lymph nodes, spleen and liver, and growth in these organs may be detected.

On physical examination, enlarged liver-spleen, body bruising and bleeding, and fever are detected. Complete blood counts show abnormalities in leukocyte count (leukocyte count may be high, low or rarely normal), anemia (decrease in red blood cells), and decrease in platelet count. The presence of blasts in peripheral smear supports the diagnosis. Bone marrow biopsy is required for definitive diagnosis. The biopsy sample is stained with special stains and examined by flow cytometry. A genetic examination is performed for the determination of chromosomal abnormalities.[7]

Asparagine is known to be consumed in high amounts by the ALL cell, so ASNase (Asparaginase) is used for the therapy of ALL. Asparaginase achieves its antileukemic impact by depleting the circulation of asparagine and removing the amino acid from the cancer cells. [8, 9, 10] Given this mechanism of action, it is thought that adequate and maintained rates of asparagine depletion are essential in achieving ideal leukemic cell death and positive patient results. [11, 12]

1.2.1.3 Other Leukemia Subtypes

Chronic lymphocytic leukemia (CLL) is a type of blood and bone marrow cancer caused by lymphocytes. It is the most common type of chronic leukemia. In 2008, 15,110 new CLL patients and approximately 90,179 living CLL patients were reported in the United States. Although CLL usually occurs at the age of 60 and over, 15% of patients are under 50 years of age. There is no statistical information about the incidence in our country. [13]

A lymphocyte that becomes a cancer cell and multiplies over time, replaces normal lymphocytes in the bone marrow and lymph nodes. These cells, unlike normal lym-

phocytes, have lost the ability to fight infection.

CLL is a type of leukemia that can go for a long time without progress, and without disturbing the patient's health. Blood tests and physical examinations are performed periodically in patients followed up without treatment. During follow-up, progress is monitored and if the stage progresses (stage II and above), or if the lymphocytes in the blood have doubled or more in the last 6 months, the presence of frequent recurrent bacterial infections, disease-related anorexia, weight loss, and night sweat develop, treatment can be initiated. [13]

In acute myeloid leukemia (AML), the normal maturation process is disrupted, the young blast cells cannot mature and begin to accumulate in the bone marrow and blood. (Figure 1.5) Since mature cells such as neutrophils and monocytes can not mature, the body is vulnerable to germs. As a result of abnormal development of myeloblasts, erythrocyte, and platelet production in the bone marrow is disrupted. Consequently, anemia and a decrease in platelet count occur. [14]

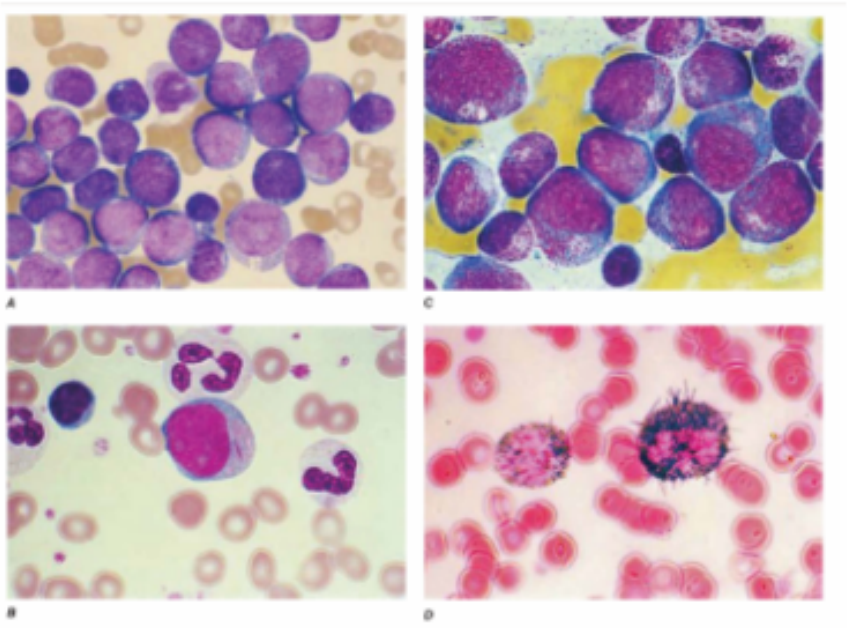

Figure 1.5: Acute Myeloid Leukemia Microscopy Image [1]

Most patients experience increased discomfort for weeks or even days without a significant health problem. Anorexia is common and may cause weight loss. [14]

1.3 Metabolomics

Metabolomics is a biotechnology branch that analyses particular chemical fingerprints of specific cellular and biochemical mechanisms, primarily the patterns of all small molecules formed by those same mechanisms. It promotes transcriptomic and proteomic analyses by practicing quantitative analysis of analytes of small molecular weight (< 1800Da) stating a biological system's metabolic status. While genomics and proteomics give information about what can happen in the sample, metabolomics gives information about what happens. Therefore, detailed and quantitative measurement of all metabolites (metabolomics) is the most ideal method for diagnosing a disease or investigating the effects of toxic agents on phenotype. It has formed and integrated many fields since the mid-1990s, which include diagnosis, drug studies and innovation, diet, food science, botany and toxicology, ecosystem and human health, all heavily linked to health care. [15, 16]

1.3.1 Metabolomic Techniques

Metabolomics is a multidisciplinary science involving biology, chemistry, and mathematics. Analytical techniques such as chromatography, molecular spectroscopy, and mass spectrometry combined with multivariate data analysis methods are needed. Metabolomics study is dominated by nuclear magnetic resonance (NMR) and mass spectrometry (MS), combined with various separation methods. NMR determines magnetic resonance in molecules containing hydrogen atoms, whereas MS measures ionized molecules, according to their mass-to-charge (m/z) ratios. Sample pretreatment is not required in NMR assessment. This method, however, has low sensitivity. Therefore, the most common method for metabolome measurement is the MS method combined with a previous separation technique, such as chromatography.

1.3.1.1 Liquid Chromatography Mass Spectrometry (LC-MS)

For metabolome assessment, liquid chromatography combined with mass spectrometry (LC-MS), gas chromatography combined with mass spectrometry (GC-MS), or

capillary electrophoresis combined with mass spectrometry (CE-MS) techniques are commonly used. [17]

LC-MS is widely used in metabolomics studies and is an appropriate method for analyzing non-volatile, thermally sensitive, high- or low-molecular-weight compounds. Therefore, LC-MS is suitable for the metabolomic assessment of diverse biofluids (urine, blood, etc.) [18, 19] Pre-treatment in this method is simpler and quicker in comparison to GC-MS.

Metabolite separation is usually achieved by using reverse phase column and ESI in LC-MS-based metabolomics. The gradient reverse-phase HPLC separation is intended for compounds with medium to low polarity, so it can not make hydrophilic metabolites, like amino acids or carbohydrates to adsorb properly. Hence, new column chemistries such as columns of hydrophilic interaction liquid chromatography (HILIC) have been created.[20] Additionally, dimensions of LC columns and particle diameters affect this method's sensitivity and separation power. Ultra high-performance liquid chromatography (UHPLC) is successfully used in metabolomics studies to improve chromatographic resolution. [21, 22]

A mass spectrometer can be operated in two modes, scan mode or selected ion monitoring (SIM) mode. In scanning mode, during a brief span of a moment, the tool detects signals over a mass spectrum. In the selected ion monitoring mode, the mass spectrometer can be set to track just a few mass-to-charge ratios (m/z) instead of continually scanning. As a consequence, the quadrupole can test each of the m/z values in considerably more time, with a consequent and drastic increase in the sensitivity. [23]

The most frequently encountered adducts in the positive-ion mode are Na+, K+, and NH4 +, and in the negative-ion mode are Cl, and CH3COO. Because mass-to-charge (m/z) ratios are measured in MS, multiply charged ions will be detected at lower m/z. For example, there will be a double charged ion at m/z corresponding to [M+2H]2+/2, easily recognizable by a mass difference of 0.5 Da (1 Da divided by the charge) between the monoisotope and the first isotope peak. [24]

After the scan mode, the mass spectrometer gives a Total Ion Chromatogram (TIC),

which shows all of the ions in the sample as an output. By processing the given output, we obtain Base Peak Chromatogram (BPC), which is the most abundant ions in the sample and has less noise than the TIC. On the other hand, after the selected ion monitoring mode, the mass spectrometer gives Extracted Ion Chromatogram (XIC), which shows only the selected ions. In an XIC, the intensity (counts) for the ion with the chosen m/z is plotted as a function of time. SIM is mainly used for quantification of the metabolite of interest.

In the LC/MS method, HPLC and MS units are used together for illuminating the structure and quantification.

The HPLC Unit consists of three main parts:

- LC Pump: It allows the mobile phases to be pumped in desired proportions by the back and forth movements of the pistons.
- Autosampler: Provides automatic injection of samples. It is possible to control the column furnace and sample temperature.
- PDA Detector: Works with ultraviolet and visible wavelengths. The wavelength range is 190-800 nm.

The MS can also be examined in three main parts:

- Ion Max API Source: ESI (Electrospray Ionization) or APCI (Atmospheric Pressure Ionization Source) ionization techniques may be used depending on the sample to be analyzed. In general, polar compounds such as amines, peptides, and proteins are analyzed by the ESI technique and apolar compounds such as steroids are analyzed by the APCI technique.
- Mass Analyzer: The ions from the ion source are subjected to varying electric field on the mass analyzer and separated according to m/z (mass/charge) ratios.
- MS Ion Detector System: MS detector is a high sensitivity ion detector system operating in positive and negative ion modes.

In LC-MS/MS technique, sample molecules separated according to their physicochemical properties are analyzed by a mass detector. Mass spectrometers stimulate

molecules by ionization to convert them into charged ionized molecules.

To ensure an extremely specific quantification, the targeted metabolite should be analyzed using the selected/multiple reaction monitoring (SRM/MRM) using triple quadrupole (QqQ) MS. Triple Q MS consists of three chambers, two of which are mass filters, Q1 and Q3, which allow the metabolite ion of the desired mass to pass through. The metabolite is divided into its ions in the second chamber, Q2, by collision with N2 gas. The third quadrupole filter is used to diagnose and quantify the ions (daughter ions or product ions) formed as a result of disintegration. The use of two mass filters guarantees elevated selectivity and the fusion of Q1 and Q3 chambers, called transition, enables for a single analysis of up to 300 distinct ions. [25]

Using a standard for precise measurement is essential. A stable isotope-labeled metabolite with the same molecular structure as the metabolite of interest can be differentiated from the target metabolite by the variation in mass due to the labeling. As the isotope-labeled metabolite's retention times and the target metabolite are identical, they will have the same peak. The internal standard is also needed to enhance analytical precision. [25]

When the metabolite chosen to be used as a standard is not labeled, it is called authentic standard, and this time, known-amount of the metabolite of interest is run solely at LC-MS, and after getting the resulting peak of the standard, the sample is run afterward with same conditions. This way the concentration of the metabolite of interest can be calculated by comparing the known amount of authentic standards.

1.3.2 Cancer Metabolomics

Cancer is a disorder of metabolism. Alterations in oncogenes (PTEN, RAS, ERK, etc.) and oncological transcription factors (p53, c-MYC, HIF, etc.) are influenced by a variety of metabolic enzymes that respond to the metabolic variations seen in cancer. For decades, studies have focused on cancer metabolism, the process that significantly regulates the phenotype of cancer. Intriguingly, varying cell alterations trigger likewise downstream metabolic consequences, revealing the significance of cancer cell metabolism.

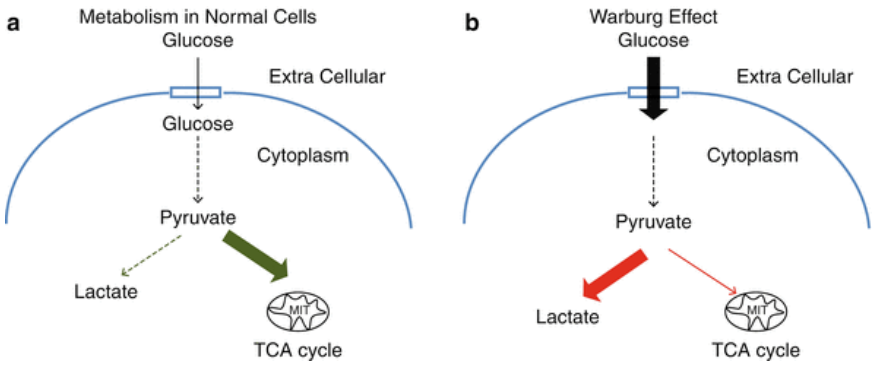

Figure 1.6: The Warburg Effect [26]

Typically, glucose transformation to lactate is increased, the synthesis of nucleic acid, enzymes, and lipid by the use of glucose and lactate are accomplished, TCA-cycle interference or disturbance is seen, ATP supply is regulated and glutathione is increased in the context of NADPH and glutathione production. (Figure 1.6) An essential trait of cancer is characterized as a changing metabolism, which is an important field to assess drug targets. [27]

Challenges that underlie the onco-metabolomic research are specimen types and analytical techniques. Plasma, serum, urine, and tissue samples are commonly included within the current metabolomic specimens. Sweat, exhaled air, bronchoalveolar lavage fluid, saliva, and other biological samples have also been reviewed in these studies [28, 29]. These samples are less damaging to patients compared to regularly used specimens, and thus are more accessible and are non-invasive samples, that may reflect a shift in the selection of samples. Same with analytical methods, there are both benefits and drawbacks in the widely used nuclear magnetic resonance [30], gas chromatography-mass spectrometry [31], and liquid chromatography-mass spectrometry [32] methodologies.

However, it is still one of the rapidly growing cancer research branches, since in many studies it can identify variations in a large number of metabolites concurrently without the need for a hypothesis. More than 2000 original study publications have been issued over the past decade on cancer metabolomics. This includes studying many cancers in varying sample groups, as cells, tissues, or body fluids, to identify metabolic markers or biomarkers. These markers have prospective use in the identi-

fication, prognosis, and diagnosis of cancer to increase sensitivity and specificity. In any scenario, varying samples can be selected as possible drug targets from human tissue fluids to animal specimens, or cell culture.

Table 1.1: Summary of the discovered oncometabolites and associated cancer types

Oncometabolites	**Related Diseases**
D-2-Hydroxyglutarate	Low-grade Glioma [33], Secondary Glioblastoma [34], Chondrosarcoma [35], Cholangiocarcinoma [36], Acute Myeloid Leukemia (AML) [37, 38]
Succinate	Hereditary Paraganglioma (PGL) Pheochromocytoma (PCC) [39]
Fumarate	Hereditary Leiomyomatosis, Renal Cell Cancer (HLRCC) [39]
Butyrate	Colorectal Cancer [40]
Choline	Prostrate Cancer [41], Breast Cancer [42]

Articles and references from previous cancer metabolism studies have increased dramatically over the past 5 years and have formed a field of their own. Nearly 400 original study publications in the field of cancer metabolomics have been written in 2015. [43, 44]

1.3.3 Metabolomics in Leukemia

An overwhelming obstacle remains to be the early diagnosis and efficient therapy of hematological malignancies. The assessment of variations in these compounds may function not only as a biomarker in diagnosis/prognosis in cases of malignancy but also as a means of controlling, treating and monitoring the disease. Many studies have recently been performed through the use of some metabolic profiles in malignant tumors including the brain, lung, prostate, pancreatic, breasts, ovaries, liver and

thyroid. [45]

In 2001, Martin Tiefenthaler and his friends showed that increased lactate levels in apoptosis-induced leukemia cells cause acute tumor-lysis syndrome due to lactate accumulation and cause organ failures [46].

In 2004, Sven Gottschalk et al. investigated the effects of imatinib on the glucose metabolism in BCR-ABL-positive and BCR-ABL-negative leukemia cell lines and showed that imatinib addition suppressed glycolytic activity and activated the Krebs cycle, thus inhibited cell proliferation [47].

In 2009, Elaine R. Mardis et al. investigated the recurring mutations in AML and found that IDH1 mutation responsible for 2-hydroxyglutarate accumulation was one of them [38]. In 2010, Stefan Gross and his friends found the specific point mutations that can be targeted [48]. And finally, in 2018, FDA announced the approval of Tibsovo (ivosidenib), the first drug in IDH1 inhibitors class [49].

Currently, the clinical diagnosis of ALL includes an arduous invasive bone marrow puncture, especially for young people. Thus, progress in diagnostic processes is necessary. To date, metabolic shifts related to ALL have not yet been evaluated. [50]

1.4 Blastic Transformation of Chronic Myeloid Leukemia (CML)

A constitutively functional fusion protein, BCR-ABL, the fusion of which is produced by t(9;22) mutation recognized as Philadelphia chromosome (Ph+), causes CML. Normally, there are 23 pairs of chromosomes in our cells, but a structural change occurs in chromosome 22 in CML. This altered 22nd chromosome is the Philadelphia chromosome, and it causes leukemia cells to increase in blood. There are three different BCR-ABL oncoprotein messages, according to the breaking points of chromosome 9 and chromosome 22. (Figure 1.7) p210 BCR-ABL1 is the most common message in CML. p190 BCR-ABL1 is present in 2/3 of patients with Ph+ ALL and rare in CML. p230BCR ABL1 is rarely seen in CML patients and rather associated with the chronic phase. How and why Philadelphia chromosome mutation occurs in blood cells is not well known. [6]

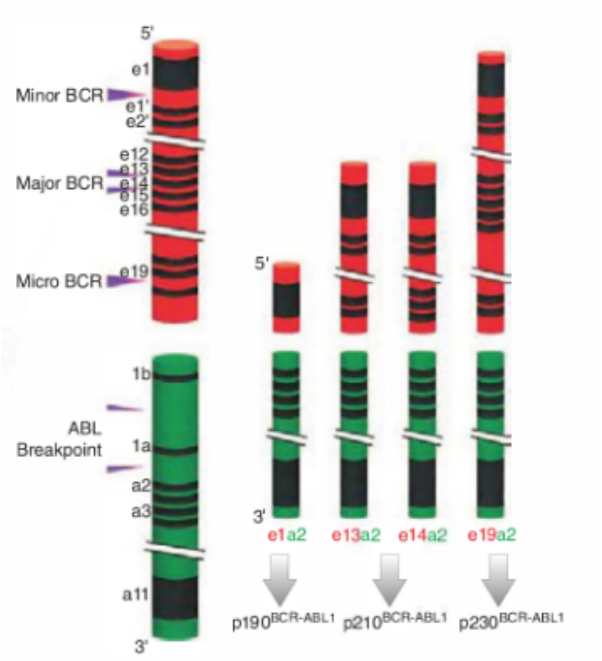

Figure 1.7: Three types of BCR-ABL messages (2013 The University of Texas MD Anderson Cancer Center)

CML typically develops in three clinical stages; a chronic stage, an accelerated period, and terminal blast stage which is an acute myeloid (AML) or a lymphoblastic

disease (ALL).

The blast phase, in which the disease turns to acute leukemia, is either myeloblastic (70%) or lymphoblastic (30%), is relatively resistant to treatment. The type of blast cells should be determined when a blast transition appears. If the leukemia is lymphoblastic rather than myeloblastic, it is easier for the disease to respond to suitable acute leukemia therapy. Since the survival depends on the timing of the blast crisis, which can not be foreseen, this is the cause of death in most patients. If the imatinib treatment was not applied, approximately 10% of patients per year would enter the blast phase. However, after 10 years of imatinib therapy, only 0.5% to 2.5% of the patients enter the blast phase.

1.5 Contributions and Novelties

Even though it is always better to diagnose the disease in earlier phases, if the disease transformed into blast phase, it would be fairly beneficial to detect the differences between the start of the blast crisis and the fully transformed disease. Since CML in blast crisis can turn into AML and ALL, finding differential indicators to have a clear diagnose to decide on the specific treatment, can save the patients life.

While there are many metabolomics-related studies on AML, ALL, CLL, and CML differentially, there none were comparing the metabolic fingerprints of ALL and CML via targeted HPLC-MS. Besides, prior studies were conducted on blood, plasma cells, and bone marrow tissues, but not on cultured cells.

Our contributions are as follows:

- This is the first study to compare metabolite differences between CML and ALL, using cultured cells unlike the similar studies that compare other leukemia types,

- Also, this study can be used as a foundation for future studies for finding a non-invasive and fast early diagnosis solution to potential CML and ALL patients.

1.6 The Aim of the Thesis

In this study, the metabolic differences of Jurkat (ALL) and K562 (CML-BP) cell lines were aimed to be evaluated using HPLC-MS towards future diagnostic studies.

Based on the knowledge that there is a significant increase/decrease in expression levels of some genes associated with carbohydrate pathways as a result of the acute transformation of CML into ALL [51, 52, 53], it is expected that a significant difference will be observed for some metabolites when samples isolated from two cell types are measured by HPLC-MS.

With the results, further studies can be applied to reveal metabolic patterns to disclose if the patient has just entered the blast crisis phase of CML, or developed ALL.

CHAPTER 2

MATERIALS AND METHODS

2.1 Chemicals

Ammonium Bicarbonate was kindly given by METU, Chemical Engineering Department. Ammonium bicarbonate stock was prepared in Milli-Q water. Internal standards citric acid and lactic acid were provided by the METU Central Laboratory, Molecular Biology and Biotechnology RD Center, Mass Spectroscopy Laboratory.

2.2 Cell Culture

The human T cell acute leukemia cell line (Jurkat - ATCC® TIB-152 lymphoblast from peripheral blood) and the human chronic myeloid leukemia (blast phase) cell line (K562 - ATCC® CCL-243, lymphoblast from bone marrow) were kindly gifted by the Hematology Service of Gülhane Military Medical Academy (GATA). Jurkat and K562 cells were cultured in RPMI 1640 medium supplemented with 10% (v/v) fetal bovine serum, 1% (v/v) penicillin-streptomycin, 1% (v/v) non-essential amino acids and 1 μg/ml plasmocin prophylactic as suspension culture, and incubated in T-25 and T-75 sterile tissue culture flasks at 37°C in 5% CO_2 with humidified Thermo Scientific (USA) incubator.

2.3 Quenching Of Cells And Metabolite Extraction

For quenching of the cell metabolism, 1 volume of cell ($1x10^7$ cells) was dispensed in 5 volume cooled quenching solution (60 (v/v) methanol, 0.85 (w/v) AMBIC (pH

7.4), -40°C). After centrifugation at 1,000g for 2min at -20°C, the supernatant was removed by aspiration and the pellet was resuspended in 500μl 100 methanol (-80°C) and snap-frozen in liquid nitrogen.

Frozen cells were thawed at room temperature (25°C), vortexed for 30 seconds and centrifuged at 800g for 2min. Its supernatant was collected at -20°C. The same procedure was repeated once more, and then, the cell pellet was resuspended in 250ul ice-cold MilliQ water, and snap-frozen in liquid nitrogen.

The suspension was thawed in room temperature (25°C), vortexed for 30 seconds and centrifuged at 15,000g for 2min. The supernatant was pooled with the methanol fractions in the tube at -20°C. The pooled supernatant fractions were centrifuged once more at 15,000g for 2min and transferred to a fresh tube. Then, the supernatant was dried using a MAXI dry lyo vacuum centrifugal evaporator at 30°C.

2.4 Triple Quadrupole (QqQ) LC-MS

Two different LC-MS procedures were conducted by the METU Central Laboratory, Molecular Biology - Biotechnology RD Center, Mass Spectroscopy Laboratory, according to parameters below, with three biological and technical replicates.

Table 2.1: Table for LC parameters of two methods. "Screening Method" indicates the regular method of METU Central Laboratory, that is used for mass-screenings in this study, and "Quantification Method" indicates the method belongs to Omar Al Kadhi et al., which is used here to determine the concentrations of lactic acid and citric acid in Jurkat and K562 cell extracts.

LIQUID CHROMATOGRAPHY		
	Screening Method	**Quantification Method**
Equipment	Agilent 1200 HPLC Series	Agilent 1200 HPLC Series
Column	Zorbax Eclipse Plus C18 HT (2.1 x 100 mm x 1.8 μm)	Zorbax Eclipse Plus C18 HT (2.1 x 100 mm x 1.8 μm)
Mobile phase	**Solvent A:** (10 %) 0,05 % Formic Acid + 5 mM Ammonium Formate **Solvent B:** (90 %) Methanol (MS grade, MERCK)	0,2% formic acid
Column Temp.	35°C	35°C
Flow	0.3 ml/min	0.4 ml/min
Run Time	13 min	13 min
Flow Mode	Isocratic	Isocratic
Injection Volume	5 μl	2 μl

Table 2.2: Table for MS parameters of two methods. "Screening Method" indicates the regular method of METU Central Laboratory, that is used for mass-screenings in this study, and "Quantification Method" indicates the method belongs to Omar Al Kadhi et al., which is used here to determine the concentrations of lactic acid and citric acid in Jurkat and K562 cell extracts.

MASS SPECTROSCOPY		
	Screening Method	**Quantification Method**
Equipment	Agilent 6460 LC-MS/MS	Agilent 6460 LC-MS/MS
Ionization Source	ESI+ Agilent Jet Stream	ESI+ Agilent Jet Stream
Pump	Agilent BinPump-SL (G1312B9)	Agilent BinPump-SL (G1312B9)
Autosampler	Agilent h-ALS-SL+ (G1367D)	Agilent h-ALS-SL+ (G1367D)
Column Compartment	Agilent G1316B 1200 Series Thermost. Col. Compart SL	Agilent G1316B 1200 Series Thermost. Col. Compart SL
Micro-degasser	Agilent G1379B 1200 Series Micro Degasser	Agilent G1379B 1200 Series Micro Degasser
Software	Agilent G3793AA MassHunter Optimizer Software	Agilent G3793AA MassHunter Optimizer Software
Nitrogen Generator	Nitrogen Generator UHPLC-MS 30	Nitrogen Generator UHPLC-MS 30
Scan Mode	MRM	MRM
Gas Temperature	350°C	200°C
Gas Flow	9 mL/min	16 L/min
Nebulizer	35 psi	50 psi
Sheath Gas Temp.	350°C	300°C
Sheath Gas Flow	9 mL/min	11 L/min
Capillary	4000 V	3000 V
Nozzle Voltage	500 V	500 V

All used standards were dissolved in 0,2% formic acid solution in water to prepare stock solutions of 0.1 mg/ml and 5mg/ml for lactic acid and citric acid, respectively. The mix of stock solutions was prepared with concentration of each compound being

5 ppm. The mix was subsequently serially diluted, giving working standard solutions with concentration ranging from 20 to 0.2 ppm that were used for construction of the calibration curves. Concentrations of standard compounds in extracts were determined from the peak areas by using the equation for linear regression obtained from the calibration curves (R2; 0.99).

Later on, the selected metabolites were also monitored by tandem MS using multiple reaction monitoring (MRM) mode. Identification was achieved based on retention time and product ions. Concentrations of the standard compounds in the extracts were determined using the peak area in the standard chromatogram.

2.5 Data Analysis

Raw data files were converted into MZ.xml format using ProteoWizard. Data files were explored, baseline correction, noise filtering, normalization were done and the raw data was analysed using MassHunter Quantitative B.06 Workstation software (Agilent Technologies, CA, US) and XCMS. The peak area of each analyte was determined, and the concentration of the analyte was calculated using the peak area of the internal standard to peak area of analyte ratio.

Graphpad was used to perform t-test to see if the concentration difference between the Jurkat and K562 cell lines were significant or not.

MetaboAnalyst was used for statistical analysis. Peaks to Pathway option in MetaboAnalyst was used to determine the possible metabolites and related pathways in the samples. Then the detected metabolites were narrowed down to 9 with literature research.

By using the product ion informations of the selected 9 metabolites, samples were analyzed via HPLC-MS/MS to check if the peaks really belong to these metabolites.

The peak areas of the metabolites were compared with the MassHunter Quantitative B.06 Workstation software (Agilent Technologies, CA, US), and a relative concentration plot was obtained with GraphPad Program.

CHAPTER 3

RESULTS

3.1 Both of the internal standards were significantly higher in ALL compared to CML-BP

Lactic acid and citric acid were chosen as authentic standards to be used as reference points for determining the concentrations the lactic acid and citric acid levels in Jurkat and K562 cell extracts, because they have key positions in cancer-related metabolisms, and the comparative amounts of metabolites found during mass screening.

3.1.1 Determination of Lactic Acid Peaks via LC-MS

5 ppm lactic acid was used as authentic standard to specifically detect the retention time of lactic acid. Then the Jurkat and K562 cell extracts were run under same conditions. The measured lactic acid concentration was evaluated by fold change via comparison of the the space under peak areas.

The chromatograms below show the peaks of both the standard and measured lactic acid in Jurkat and K562 cells. (Figure 3.1, Figure 3.2)

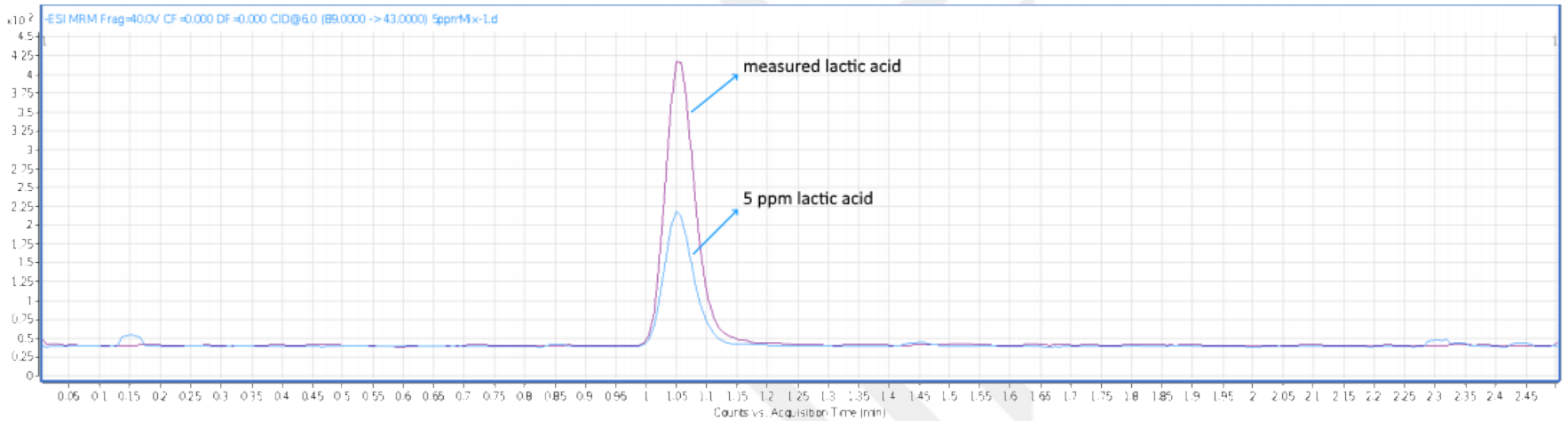

Figure 3.1: Lactic Acid Level in Jurkat Cell Extracts. At this XIC, the green peak shows the authentic standard lactic acid and the red peak shows the measured lactic acid in Jurkat cell extract.

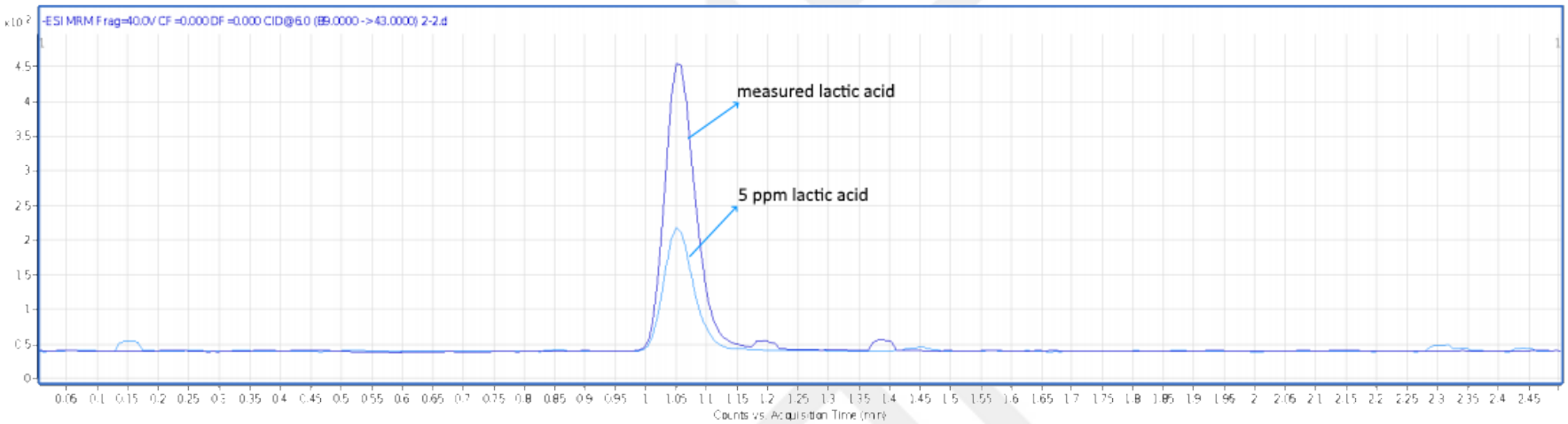

Figure 3.2: Lactic Acid Level in K562 Cell Extracts. At this XIC, the green peak shows the authentic standard lactic acid and the blue peak shows the measured lactic acid in K562 cell extract.

3.1.2 Determination of Citric Acid Peaks via LC-MS

5 ppm citric acid was used as authentic standard to specifically detect the retention time of citric acid. Then the Jurkat and K562 cell extracts were run under same conditions. The measured citric acid concentration was evaluated by fold change via comparison of the the space under peak areas.

The extracted ion chromatogram (XIC) below show the peaks of both the standard and measured citric acid in Jurkat and K562 cells. (Figure 3.3, Figure 3.24)

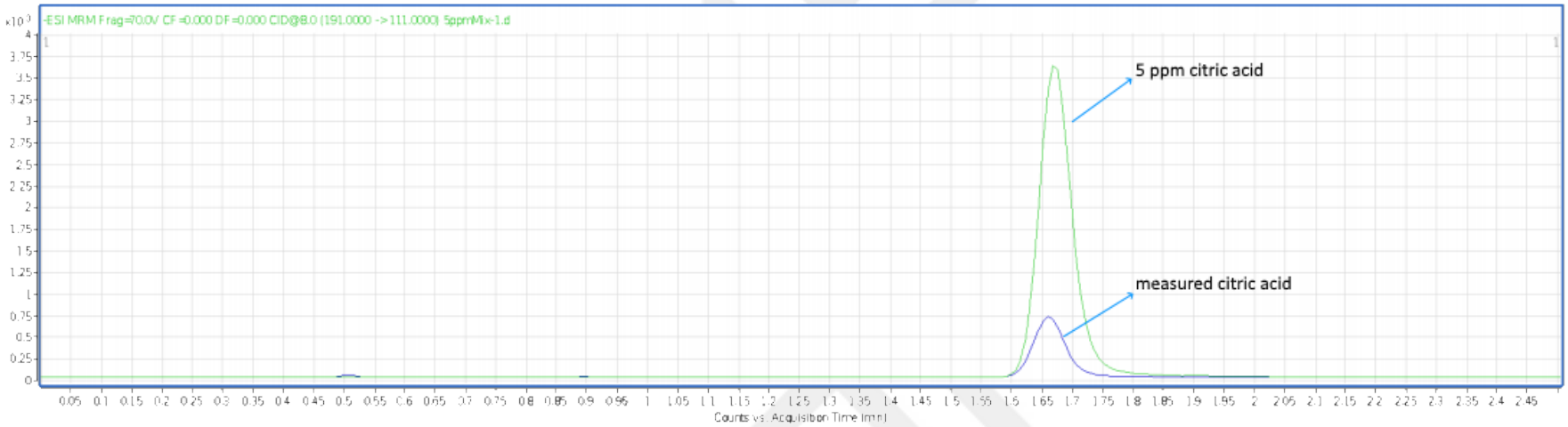

Figure 3.3: Citric Acid Level in Jurkat Cell Extract. At this XIC, the green peak shows the authentic standard citric acid and the purple peak shows the measured citric acid in Jurkat cell extract.

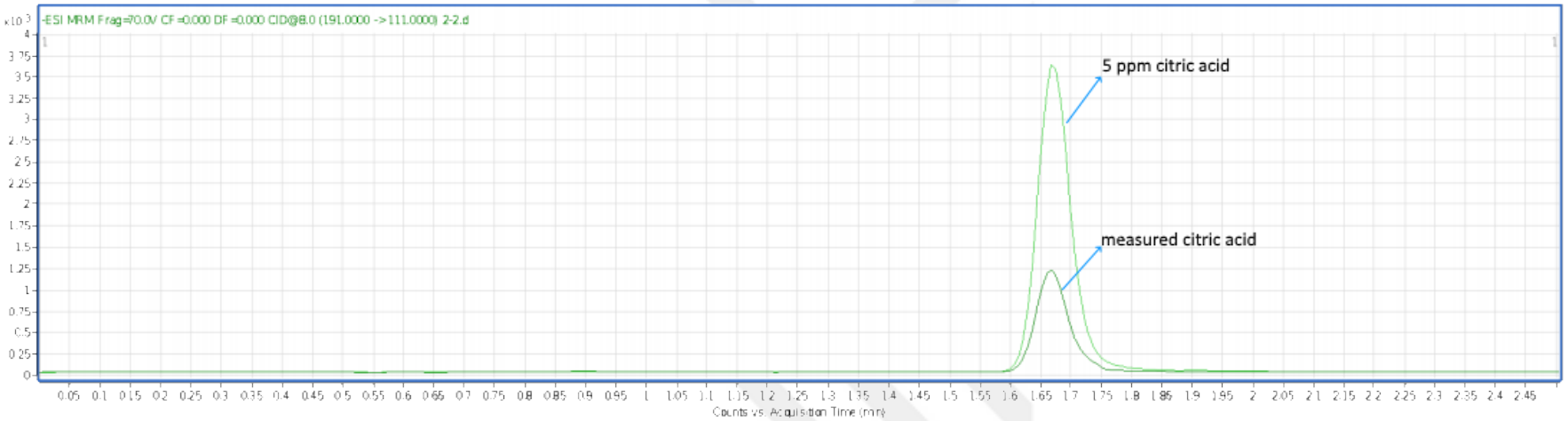

Figure 3.4: Citric Acid Level in K562 Cell Extract. At this XIC, the green peak shows the authentic standard citric acid and the blue peak shows the measured citric acid in K562 cell extract.

3.2 Calculation of the Concentrations of Lactic Acid and Citric Acid

The peak areas of lactic acid and citric acid were determined and the concentration of them was calculated using the peak area ratio (peak area of the analyte/peak area of the authentic standard) at extracted ion chromatogram (XIC) below.

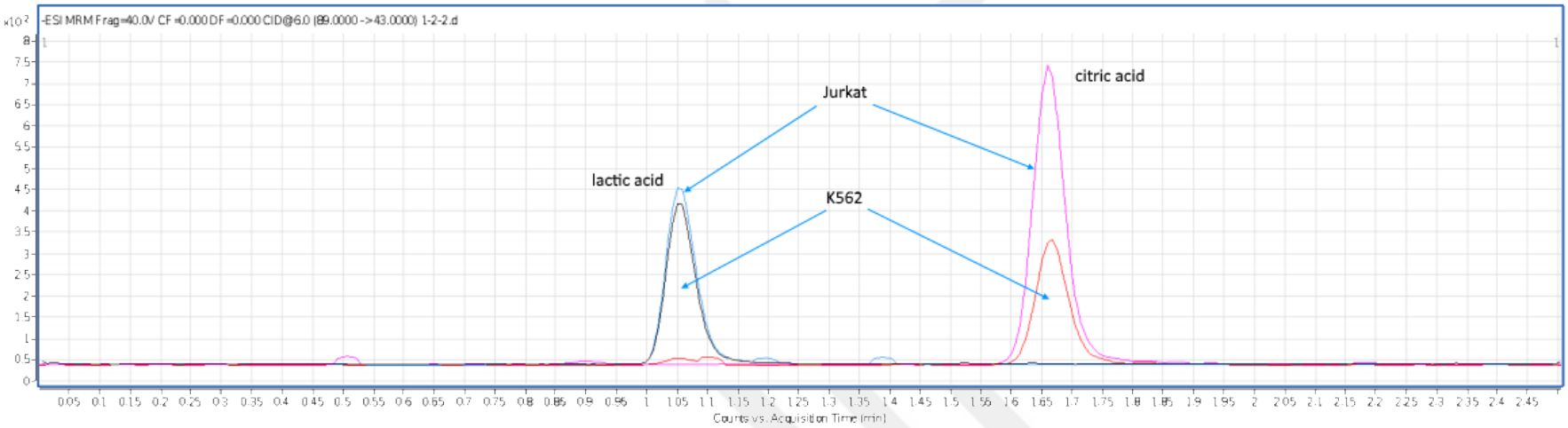

Figure 3.5: Combined Lactic Acid and Citric Acid Levels in Jurkat and K562 Cell Extracts. At this XIC, the purple and red peaks show the lactic acid and citric acid levels in K562 cell extracts, respectively. The green and pink peaks show the lactic acid and citric acid levels in Jurkat cell extracts, respectively.

In the table below, you can see the calculated lactic acid and citric acid levels.

Table 3.1: Lactic Acid and Citric Acid Readings. J-1, J-2, and J-3 indicating three readings for Jurkat and K-1, K-2, and K-3 indicating three readings for K562.

Sample No.	**Measured Concentrations (ppm)**	
	Lactic Acid	**Citric Acid**
J-1	26.94	1.91
J-2	27.36	1.92
J-3	27.78	1.93
K-1	18.30	1.65
K-2	18.12	1.65
K-3	17.95	1.64

3.3 t-test shows that the concentration difference between Jurkat and K562 cell lines is significant

Since metabolite concentration in two different types of cells are evaluated, two-sample unpaired t-test is used to define the significance of the difference.

$$t = \frac{\overline{x}_1 - \overline{x}_2}{\sqrt{s^2 \left(\frac{1}{n_1} + \frac{1}{n_2}\right)}} \tag{31}$$

$$s^2 = \frac{\sum_{i=1}^{n_1} (x_i - \overline{x}_1)^2 + \sum_{j=1}^{n_2} (x_j - \overline{x}_2)^2}{n_1 + n_2 - 2} \tag{32}$$

For lactic acid the significance in difference between Jurkat and K562 is calculated as follows,

$$\begin{aligned}
\overline{X_1} &\approx 27.36 \\
\overline{X_2} &\approx 18.125 \\
S_{X_1}^2 &= \frac{1}{n-1}\sum_{i=1}^{n}\left(X_{1i}-\overline{X_1}\right)^2 \approx 0.1764 \\
S_{X_2}^2 &= \frac{1}{n-1}\sum_{i=1}^{n}\left(X_{2i}-\overline{X_2}\right)^2 \approx 0.0307 \\
S_{X_1X_2} &= \sqrt{\frac{1}{2}\left(S_{X_1}^2+S_{X_2}^2\right)} \approx 0.3218
\end{aligned} \tag{33}$$

After substituting these values into the formula for t value is obtained.

$$t = \frac{\overline{X_1}-\overline{X_2}}{S_{X_1X_2}\cdot\sqrt{\frac{2}{n}}} = \frac{27.36-18.125}{0.3218\cdot\sqrt{\frac{2}{3}}} \approx 35.1477 \tag{34}$$

$$d.o.f = 2n-2 = 2\cdot 3-2 = 4 \tag{35}$$

The critical value for t is determined with d.o.f = 4 and $(\alpha) = 0.05$.

The critical value is 2.776 (see Appendix B).

The calculated t exceeds the critical value (35.1477>2.776), so the means are significantly different.

For citric acid the significance in difference between Jurkat and K562 is calculated as follows,

$$\begin{aligned}
\overline{X_1} &\approx 1.92 \\
\overline{X_2} &\approx 1.6467 \\
S_{X_1}^2 &= \frac{1}{n-1}\sum_{i=1}^{n}\left(X_{1i}-\overline{X_1}\right)^2 \approx 0.0001 \\
S_{X_2}^2 &= \frac{1}{n-1}\sum_{i=1}^{n}\left(X_{2i}-\overline{X_2}\right)^2 \approx 0.0001 \\
S_{X_1X_2} &= \sqrt{\frac{1}{2}\left(S_{X_1}^2+S_{X_2}^2\right)} \approx 0.01
\end{aligned} \tag{36}$$

After substituting these values into the formula for t value is obtained.

$$t = \frac{\overline{X_1}-\overline{X_2}}{S_{X_1X_2}\cdot\sqrt{\frac{2}{n}}} = \frac{1.92-1.6467}{0.01\cdot\sqrt{\frac{2}{3}}} \approx 33.4764 \tag{37}$$

The degrees of freedom is:

$$d.o.f = 2n-2 = 2\cdot 3-2 = 4 \tag{38}$$

The critical value for t is determined with d.o.f = 4 and $(\alpha) = 0.05$.

The critical value is 2.776 (see Appendix B).

The calculated t exceeds the critical value (33.4764>2.776), so the means are significantly different.

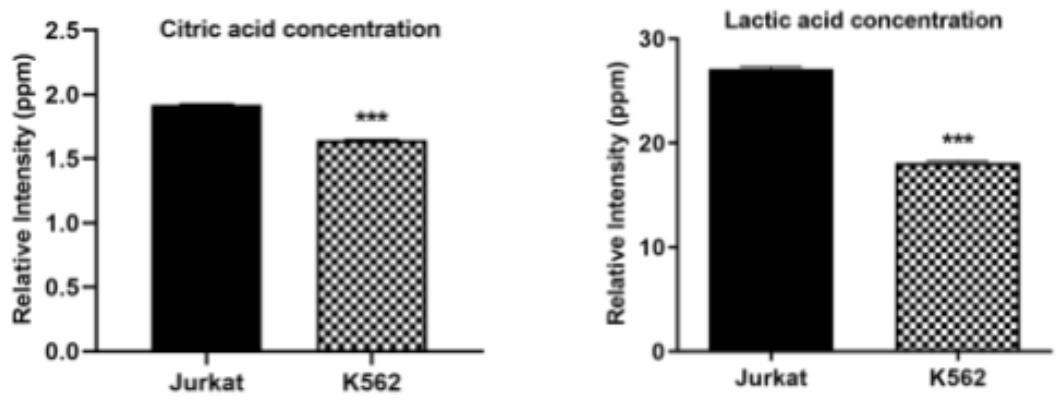

Figure 3.6: Bar plots for the relative concentrations of the lactic acid and citric acid concentrations. Each column represents the Mean+/-SEM (n=2). Asterisk *** ($p<0.001$) denote statistical significance between the concentrations of lactic acid and citric acid in Jurkat and K562 cell extracts.

GraphPad was used to perform t-test to see if the concentration difference between the Jurkat and K562 cell lines were significant or not.

The t-test showed that concentrations of both of the internal standards, lactic acid and citric acid, were significantly higher at ALL cell line, Jurkat.

3.4 3-Chlorotyrosine was absent in both cell lines in the mass scan

When the peaks were evaluated, we did not see any peaks indicating 3-Chlorotyrosine is present in the samples.

3.5 The peak-lists obtained after the mass screening gives information about active pathways

We have used two different methods for ESI mass screening to compare and select a better fitting method for cleaner peaks and more metabolites (Table 2.1 and Table 2.2).

For mass screening, the method used in lactic acid and citric acid analysis (Table 2.2) was studied in the same device in MS2Scan mode.

The resulting peaks indicate the most abundant ions in mass screening, and were then used as an input for the Peaks to Pathways feature of MetaboAnalyst online platform.

3.5.1 Jurkat Cell Line Mass Screening

Peak lists and base peak chromatograms (BPC) were obtained by scanning the of Jurkat cell extracts via mentioned methods. These BPCs show the ion counts at different m/z values.

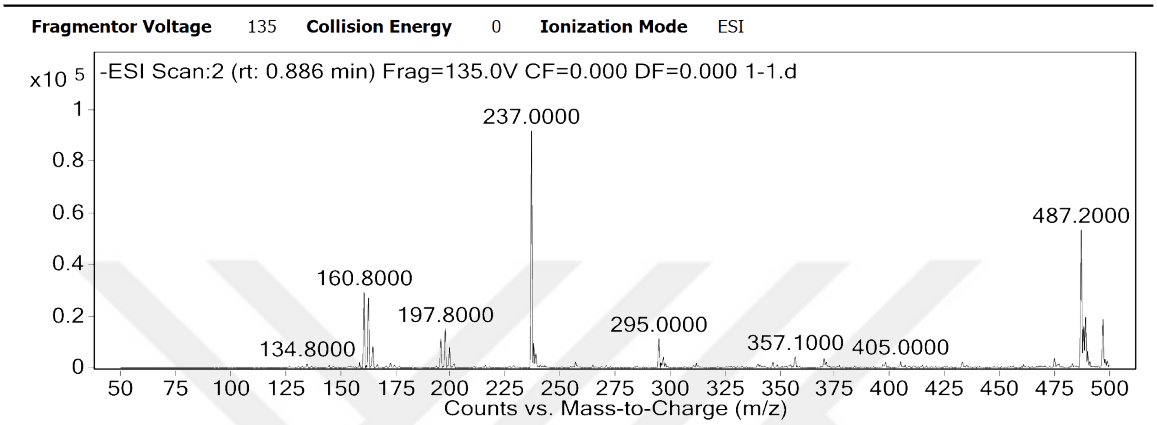

Figure 3.7: BPC of Jurkat cells obtained by Negative ESI Scan with the "Quantification Method" [54]

Table 3.2: List of peaks obtained by Negative ESI Scan of Jurkat cells with the "Quantification Method" [54]

m/z	z	Abundance
160.8	1	29138.48
162.8	1	27077.36
195.7	2	11009.10
197.8	1	14905.84
237.0	1	91789.87
295.0		11145.36
487.2	1	53400.95
488.2	1	16009.32
489.2	1	19523.12
497.1		18498.10

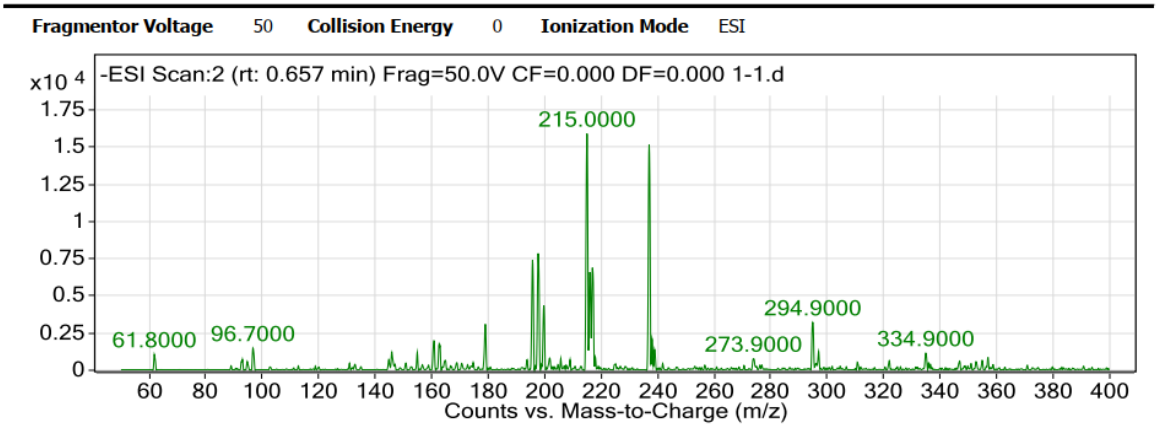

Figure 3.8: BPC of Jurkat cells obtained by Negative ESI Scan with the "Screening Method"

Table 3.3: List of peaks obtained by Negative ESI Scan of Jurkat cells with "Screening Method"

m/z	z	Abundance
179.0		3098.46
195.7	1	7400.64
197.7	1	7851.38
199.7	2	4360.44
215.0		15895.22
216.0		6589.98
216.9	1	6887.84
237.0	1	15159.46
238.0	1	2113.00
294.9		3216.18

Similar peaks were obtained using both the Quantification Method and Screening Method in the negative screenings of Jurkat cell line.

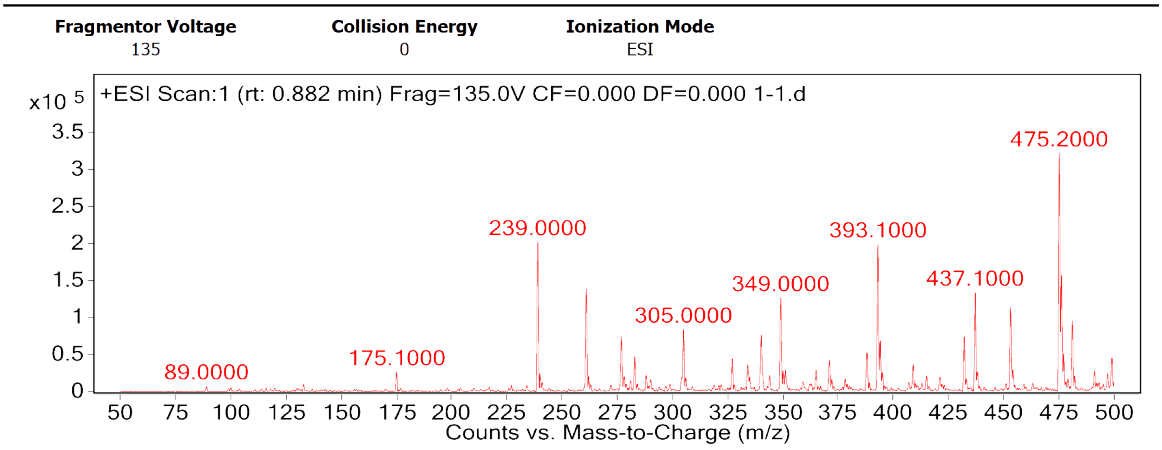

Figure 3.9: BPC of Jurkat cells obtained by Positive ESI Scan with the "Quantification Method"

Table 3.4: List peaks obtained by Positive ESI Scan of Jurkat cells with "Quantification Method"

m/z	z	Abundance
239.0		201535.53
261.0	1	138571.06
305.0		83458.97
349.0		126025.35
393.1	1	198643.75
437.1	1	133442.47
453.1		112705.11
475.2	1	321423.03
476.2	1	157216.19
481.1		95160.23

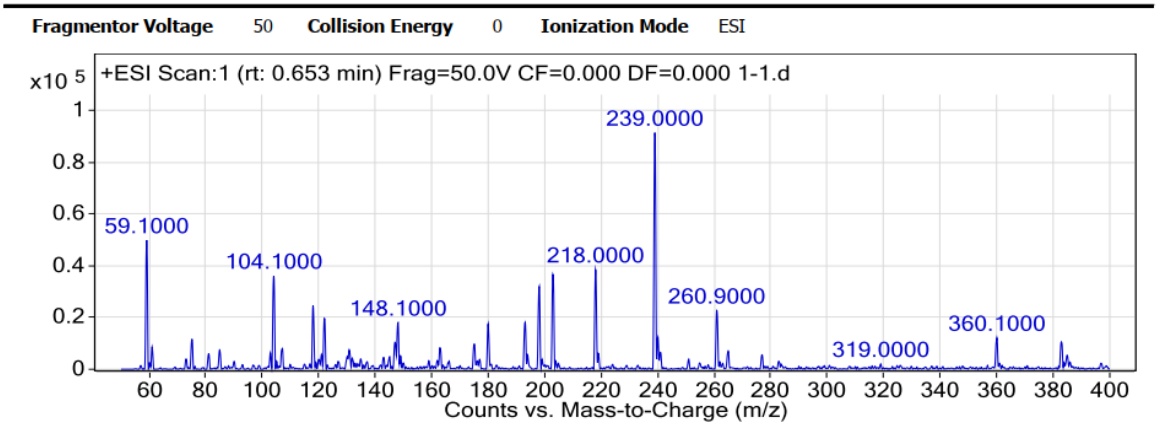

Figure 3.10: BPC of K562 cells obtained by Positive ESI Scan with the "Screening Method"

Table 3.5: List of peaks obtained by Positive ESI Scan of Jurkat cells with "Screening Method"

m/z	z	Abundance
59.1	1	49903.70
104.1	1	36148.78
118.0	1	24712.38
122.0		19678.98
193.1		18177.72
198.1	1	32023.92
202.9	1	36692.40
218.0	1	38559.12
239.0		91444.83
260.9		22723.70

Similar peaks were obtained using both the Quantification Method and Screening Method in the positive screenings of Jurkat cell line.

3.5.2 K562 Cell Line ESI Scan

Peak lists and screening graphs were obtained by scanning the of K562 cell extracts via mentioned methods. These BPCs show the ion counts at different m/z values.

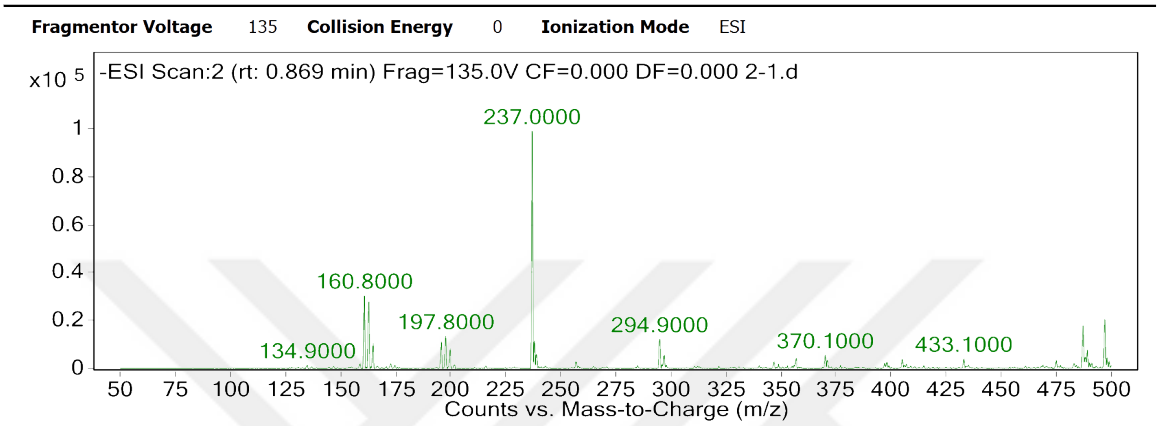

Figure 3.11: BPC of K562 cells obtained by Negative ESI Scan with the "Quantification Method"

Table 3.6: List of peaks obtained by Negative ESI Scan of K562 cells with "Quantification Method"

m/z	z	Abundance
160.8		30296.26
162.9		27682.60
164.8		10140.80
195.8		10890.06
197.8	1	13376.14
237.0		98839.20
238.1		11189.76
294.9		12134.78
487.2	1	17809.18
497.1	1	20256.12

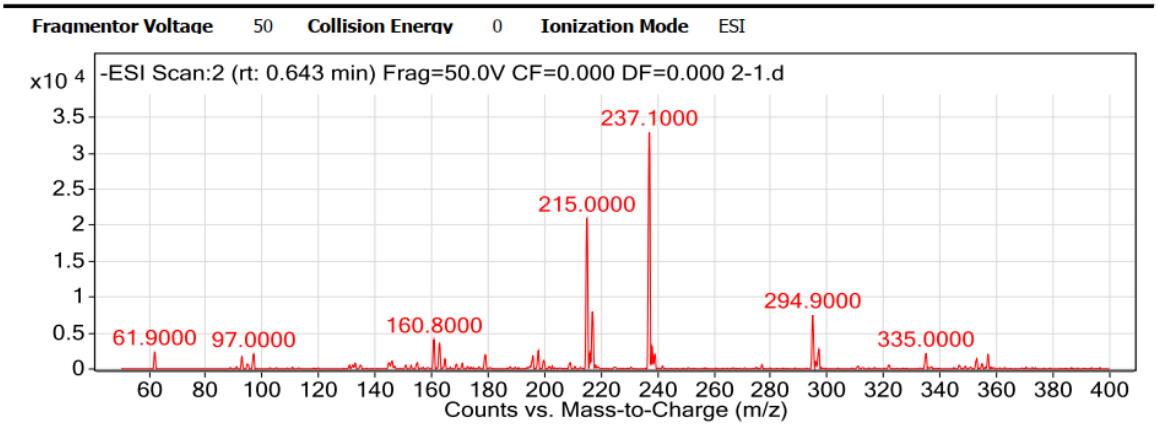

Figure 3.12: BPC of K562 cells obtained by Negative ESI Scan with the "Screening Method"

Table 3.7: List of peaks obtained by Negative ESI Scan of K562 cells with "Screening Method"

m/z	z	Abundance
61.9		2369.90
160.8		4089.16
162.8		3578.10
197.8		2571.84
215.0	1	20943.12
216.9		7977.20
237.1		32938.44
238.0		3123.76
294.9	1	7500.72
297.1		2734.92

Similar peaks were obtained using both the Quantification Method and Screening Method in the negative screenings of K562 cell line.

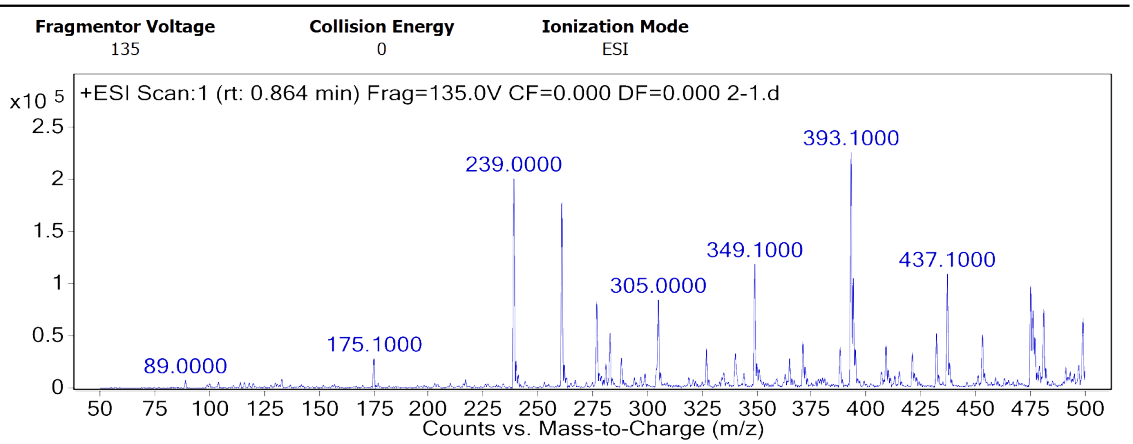

Figure 3.13: BPC of K562 cells obtained by Positive ESI Scan with the "Quantification Method"

Table 3.8: List of peaks obtained by Positive ESI Scan of K562 cells with "Quantification Method"

m/z	z	Abundance
239.0		201080.52
261.0	1	177348.30
276.9		83246.73
305.0		84638.06
349.1	1	118798.03
393.1	1	226229.45
394.1	1	105464.27
437.1	1	109546.91
475.2		98386.13
481.1	1	75817.41

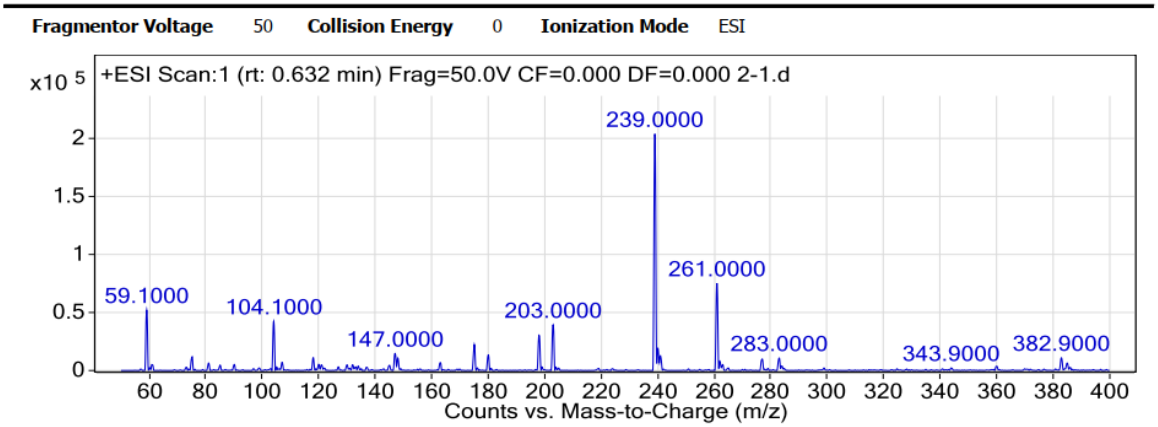

Figure 3.14: BPC of K562 cells obtained by Positive ESI Scan with the "Screening Method"

Table 3.9: List of peaks obtained by Positive ESI Scan of K562 cells with "Screening Method"

m/z	z	Abundance
59.1		52043.88
104.1	1	42320.72
147.0		14592.18
175.1		22290.82
180.1		13297.30
198.0	1	30240.14
203.0	1	39263.02
239.0		203436.52
240.1		19156.12
261.0	1	75015.60

Similar peaks were obtained using both the Quantification Method and Screening Method in the positive screenings of K562 cell line.

3.5.3 Peaks to Pathways program gave information about potential metabolites and significantly affected pathways in Jurkat and K562 cell lines

The Peaks to Pathways program uses peak lists (Table 3.2 to Table 3.9) to assess possible metabolites to related m/z values, and performs a Metabolite Set Enrichment Analysis (MSEA) and gives a plot that indicates the most significantly affected pathways in the samples.

Table 3.10: Table of metabolites obtained via Peaks to Pathways program.

m/z	KEGG ID	Ion	HMDB	Metabolites	Formula
261.0	C00072	M+HCOOK[1+]	HMDB0000044	Ascorbic acid	C6H8O6
261.0	C02670	M+HCOOK[1+]	HMDB0006355	D-Glucurono-6,3-lactone	C6H8O6
261.0	C04053	M+HCOOK[1+]		5-Dehydro-4-deoxy-D-glucuronate	C6H8O6
261.0	C04349	M+HCOOK[1+]		(4S)-4,6-Dihydroxy-2,5-dioxohexanoate	C6H8O6
261.0	C04471	M+HCOOK[1+]		(4S,5S)-4,5-Dihydroxy-2,6-dioxohexanoate	C6H8O6
393.1	C04333	M+HCOONa[1+]		Difructose anhydride I	C12H20O10
393.1	C04420	M+HCOONa[1+]		D-Fructofuranose 1,2':2,3'-dianhydride	C12H20O10
394.1	C00513	M-HCOOK+H[1+]		CDP-glycerol	C12H21N3O13P2
437.1	C00019	M+K[1+]	HMDB0001185	S-Adenosylmethionine	C15H23N6O5S
437.1	C01314	M+HCOONa[1+]		(S)-N-[3-(3,4-Methylenedioxyphenyl)-2-(mercaptomethyl)-1-oxoprolyl]-(S)-alanine	C16H20N2O6S
481.1	C03187	M-HCOONa+H[1+]		dTDP-6-deoxy-beta-L-talose	C16H26N2O15P2
481.1	C03442	M-HCOONa+H[1+]		dTDP-L-dihydrostreptose	C16H26N2O15P2
481.1	C03515	M+H2O+H[1+]		Luteolin 7-O-glucuronide	C21H18O12
237.0	C01036	M+Cl37[-]	HMDB0002052	Maleylacetoacetic acid	C8H8O6
237.0	C01061	M+Cl37[-]	HMDB0001268	4-Fumarylacetoacetic acid	C8H8O6
487.2	C01593	M-H2O-H[-]		Limonoate	C26H34O10
487.2	C02027	M-H+O[-]		Deoxylimonate	C26H32O8
497.1	C03646	M-H[-]		Oxidized gamma-glutamylcysteine	C16H26N4O10S2
175.1	C00062	M(S34)-H[-]	HMDB0000517	L-Arginine	C6H14N4O2
175.1	C00062	M(Cl37)-H[-]	HMDB0000517	D-Arginine	C6H14N4O2
175.1	C00792	M(S34)-H[-]	HMDB0003416	D-Arginine	C6H14N4O2
175.1	C00792	M(Cl37)-H[-]	HMDB0003416	D-Arginine	C6H14N4O2
175.1	C02385	M(S34)-H[-]		Arginine	C6H14N4O2
175.1	C02385	M(Cl37)-H[-]		Arginine	C6H14N4O2
198.0	C01044	M+Cl37[-]		N-Formyl-L-aspartate	C5H7NO5
203.0	C00250	M+K-2H[-]	HMDB0001545	Pyridoxal	C8H9NO3
203.0	C03493	M+K-2H[-]		D-4-Hydroxyphenylglycine	C8H9NO3
203.0	C03986	M+K-2H[-]		3-Hydroxy-4-methylanthranilate	C8H9NO3
203.0	C04324	M(S34)-H[-]		2-Hydroxy-4-carboxyhexa-2,4-dienedioate	C7H6O7
203.0	C04324	M(Cl37)-H[-]		2-Hydroxy-4-carboxyhexa-2,4-dienedioate	C7H6O7
239.0	C00331	M+K-2H[-]		Indolepyruvate	C11H9NO3
240.1	C03592	M-H[-]	HMDB0002224	5-Methyldeoxycytidine	C10H15N3O4
261.0	C04188	M(S34)-H[-]	HMDB0000963	5-Methylthioribose 1-phosphate	C6H13O7PS
261.0	C04188	M(Cl37)-H[-]	HMDB0000963	5-Methylthioribose 1-phosphate	C6H13O7PS

3.5.3.1 MSEA plots showed the related pathways to the detected metabolites

The Metabolite Set Enrichment Analysis (MSEA) shows the most significantly affected pathways in samples. Colors of the circles imply levels of statistical significance, with darker colors (up to red) mean small p-values, while lighter colors (down to white) mean larger p-values. Larger circles denote a more highly impacted metabolic pathway and smaller ones denote less impacted pathways.

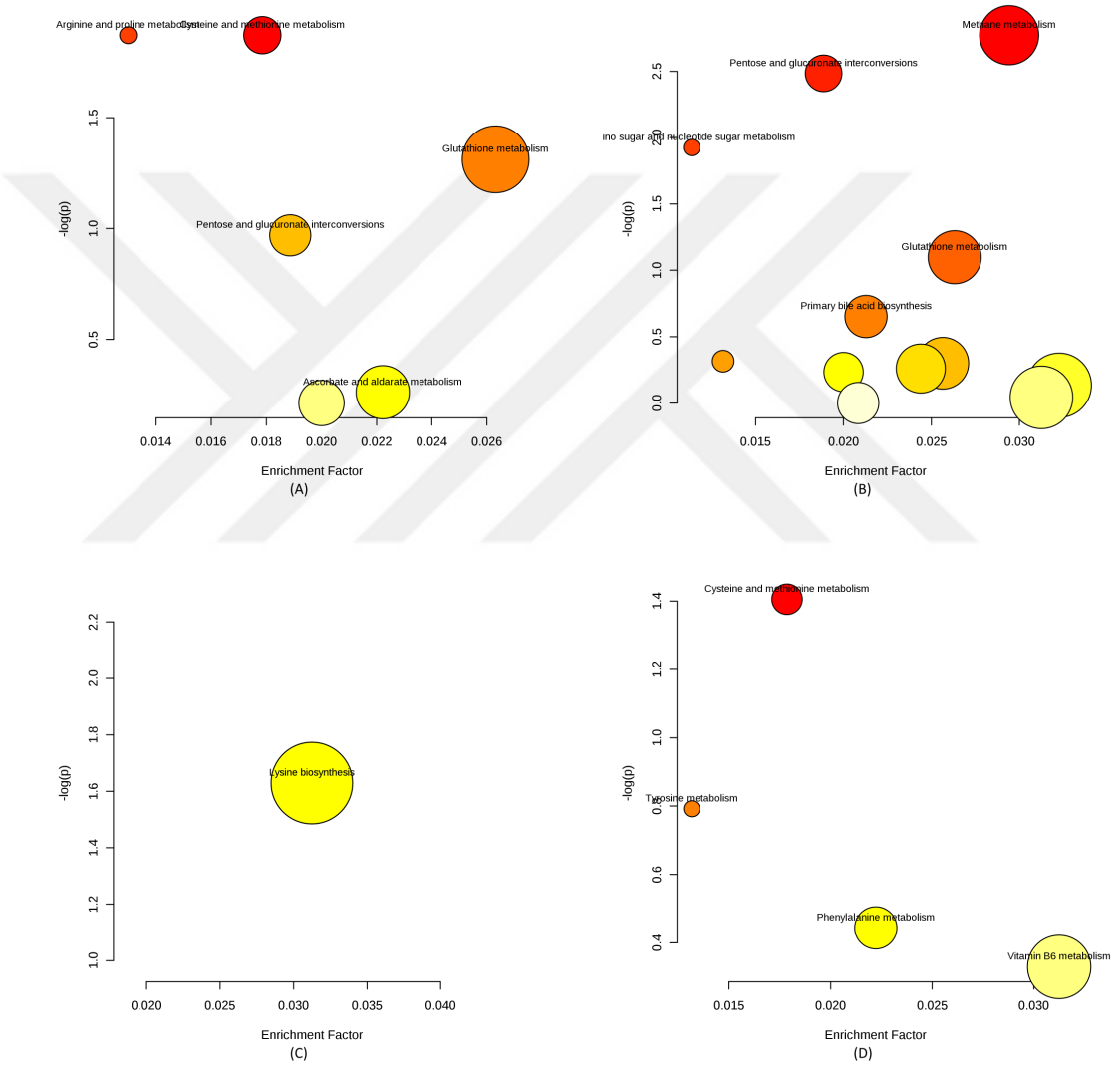

Figure 3.15: MSEA plots showing significant pathways in Jurkat Cell Line. (A) Positive screening with the Quantification Method, (B) negative screening with the Quantification Method, (C) positive screening with the Screening Method, and (D) negative screening with the Screening Method.

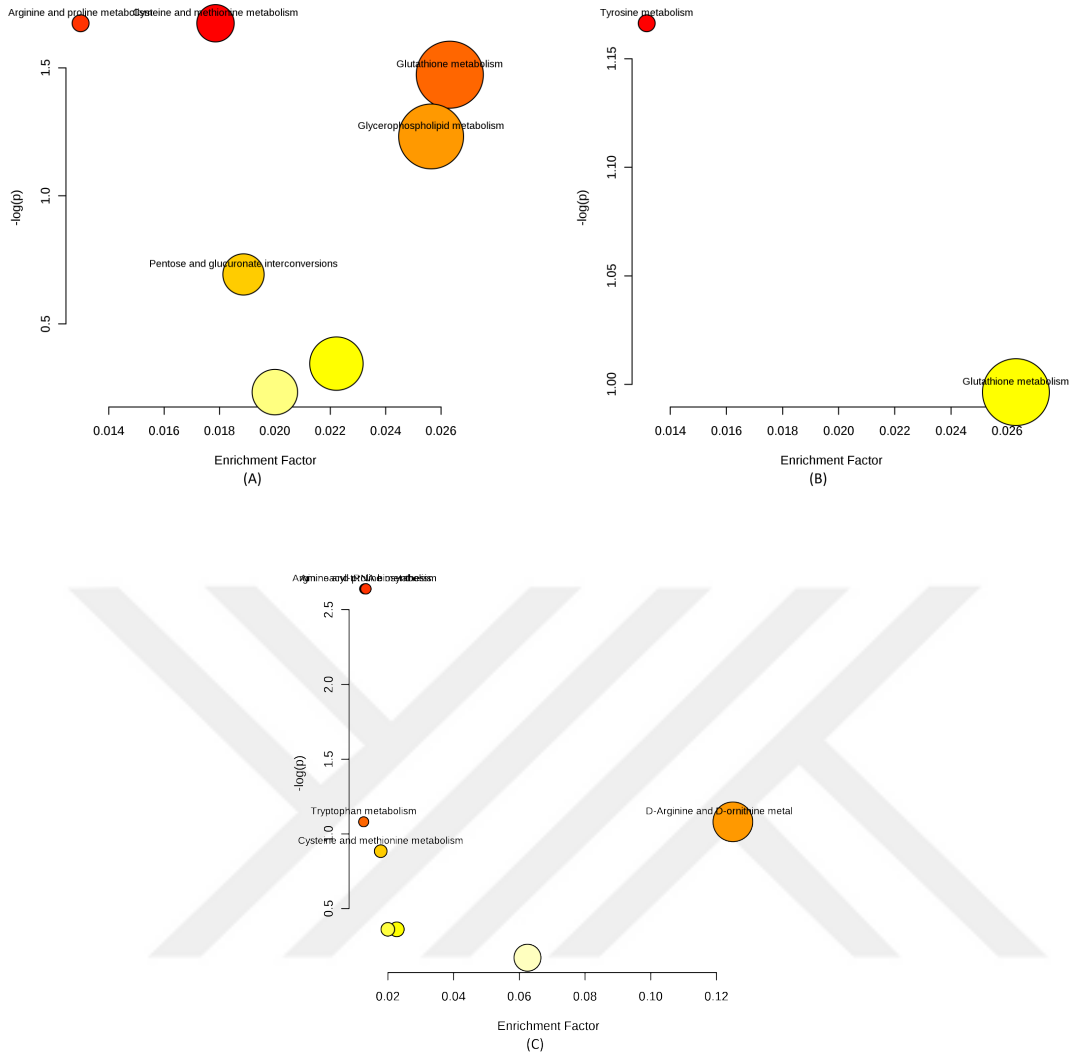

Figure 3.16: MSEA plots showing significant pathways in K562 Cell Line. (A) Positive screening with the Quantification Method, (B) negative screening with the Quantification Method, (C) positive screening with the Screening Method.

The resulting plot indicated that tyrosine, arginine and proline, and glutathione metabolisms are the main metabolisms in both cell lines.

3.5.4 Concentrations of selected metabolites were estimated by the peak area via MS/MS

After obtaining 127 estimated metabolites from the Peaks to Pathways program on MetaboAnalyst online platform, and down-scaling these to 42 with the help of the Metabolite Set Enrichment Analysis, an literature study was conducted to focus on 9 metabolites related to CML and ALL.

Table 3.11: Table of metabolites decided on further analysis via literature search, and experimental product ions of these metabolites at different collision energies found using METLIN and HMDB platforms.

Metabolite Name	Monoisotopic Mass	Average Mass	10 V POSITIVE	20 V POSITIVE	40 V POSITIVE	10 V NEGATIVE	20 V NEGATIVE	40 V NEGATIVE
Maleylacetoacetic acid	200,0321	200,1455	183,0293; 165,0188; 157,0501; 155,0344	141,0188; 139,0395; 137,0239	99,0082; 97,0290; 95,0133; 68,9977; 71,0133; 43,0184	-	-	-
4-Fumarylacetoacetic acid	200,0321	200,1455	183,0293; 165,0188; 157,0501; 155,0344	141,0188; 139,0395; 137,0239	99,0082; 97,0290; 95,0133; 68,9977; 71,0133; 43,0184	-	-	-
L-Arginine	174,1117	174,201	-	-	-	-	131,0817; 136,1390; 137,0244; 173,0200; 173,0315	-
Ascorbic acid	176,0321	176,124	177,0399; 159,0293; 99,0082; 101,0239; 103,0395	-	75,0446; 73,0290; 61,0290; 57,0340; 55,0184; 43,0184	-	-	-
S-Adenosylmethionine	399,1451	399,445	-	90,9000; 97,1000; 102,1000; 250,4000	136,0618; 119,0352	-	-	-
3-Mercaptopyruvic acid	119,9881	120,127	120,9954; 102,9848	74,9899	58,9950; 56,9793	-	-	-
5-Methylthioribose 1-phosphate	260,012	260,202	103,0218	98,9847	75,0268; 101,0061	-	-	-
Glucose 1-phosphate	260,0297	260,1358	98,9847	-	80,9742; 59,0133	-	-	-
N-formyl L aspartate	161,0324	161,1128	144,0291; 162,0397; 132,0291; 116,0342	116,0342; 102,0186; 88,0393; 86,0237; 74,0237; 72,0080	59,0128; 71,028; 70,0287; 86,0237	-	-	-

3.5.5 Evaluation of Fold Changes of Selected Metabolites in CML-BP and ALL cells

At the selected ion chromatograms (XICs) below, the peak areas of each metabolite were determined and the comparative intensity (counts) of them was calculated in both cell lines using the peak area ratio (peak area of the analyte in K562/peak area of the analyte in Jurkat).

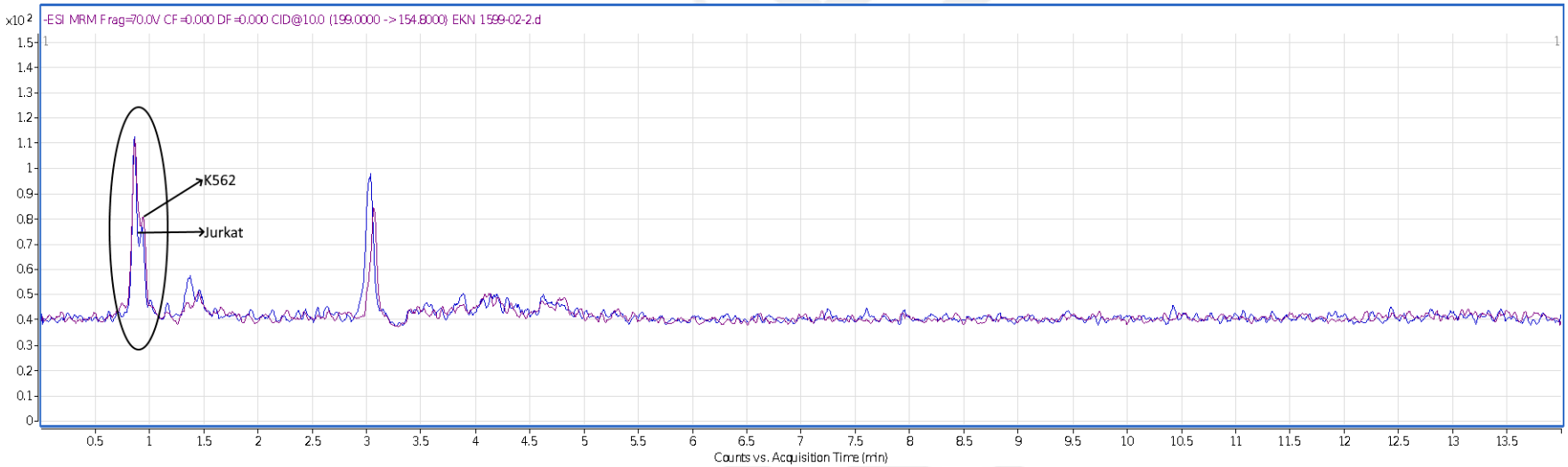

Figure 3.17: Comparative 4-Fumarylacetoacetic acid Levels in Cell Extracts. At this XIC, the purple peak shows K562 cell line and the blue peak shows the Jurkat cell line.

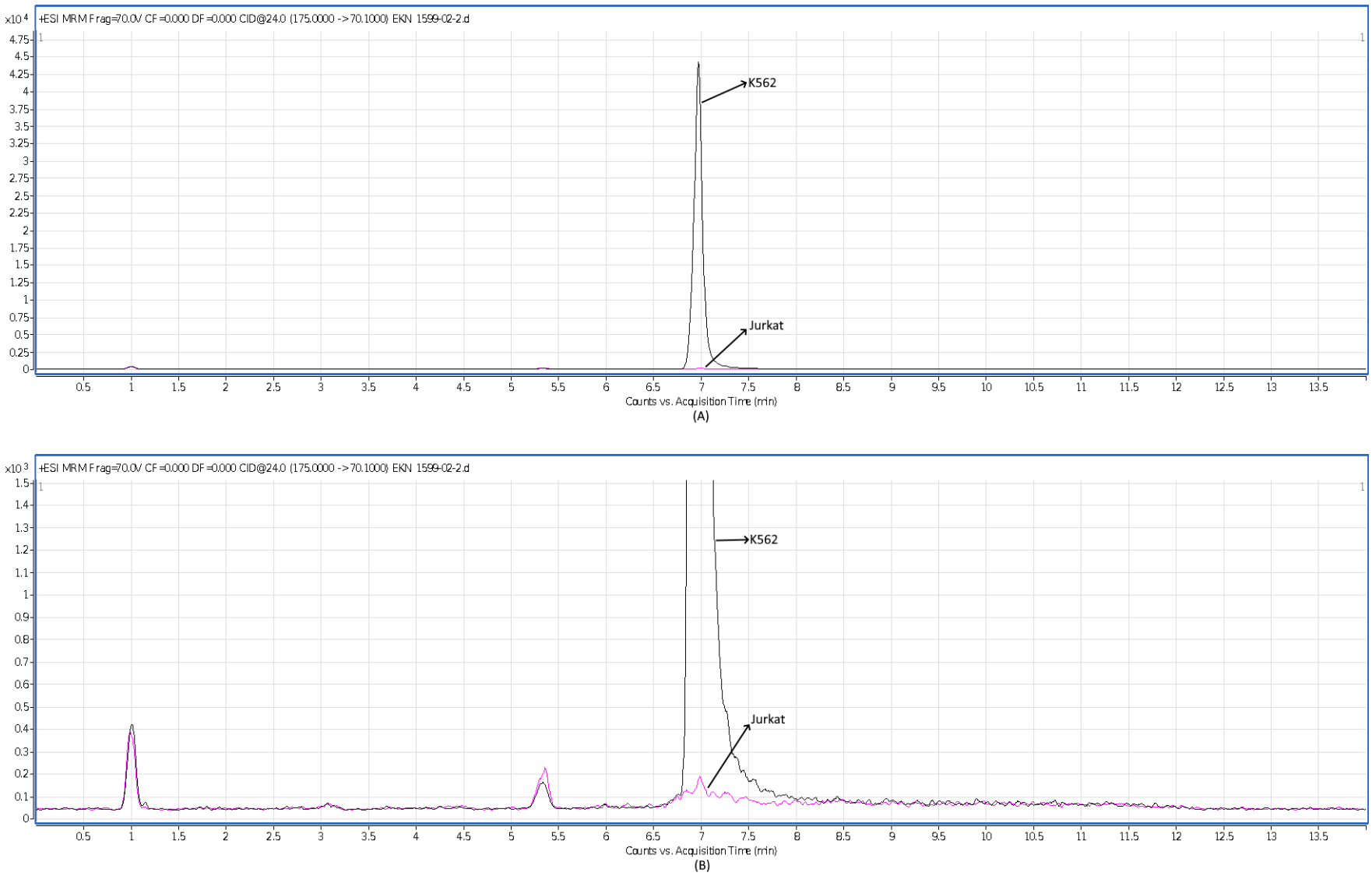

Figure 3.18: Comparative L-Arginine Level in Cell Extracts. At this XIC, (A) the black peak shows K562 cell line and the pink peak shows the Jurkat cell line (B) with its close-up figure

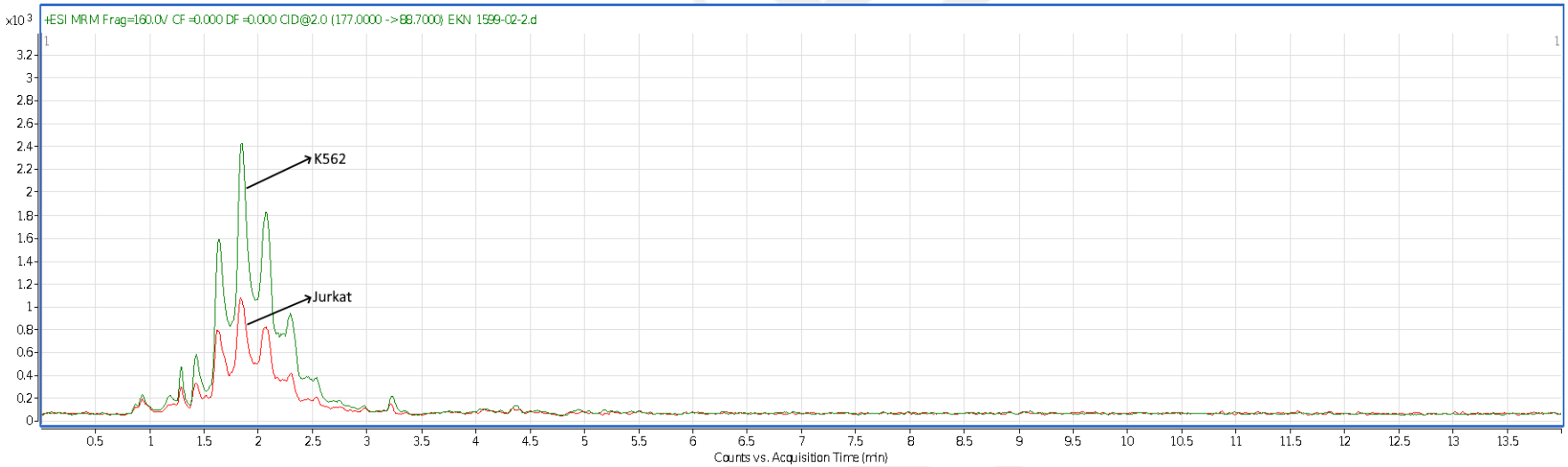

Figure 3.19: Comparative Ascorbic Acid Level in Cell Extracts. At this XIC, the green peak shows K562 cell line and the red peak shows the Jurkat cell line.

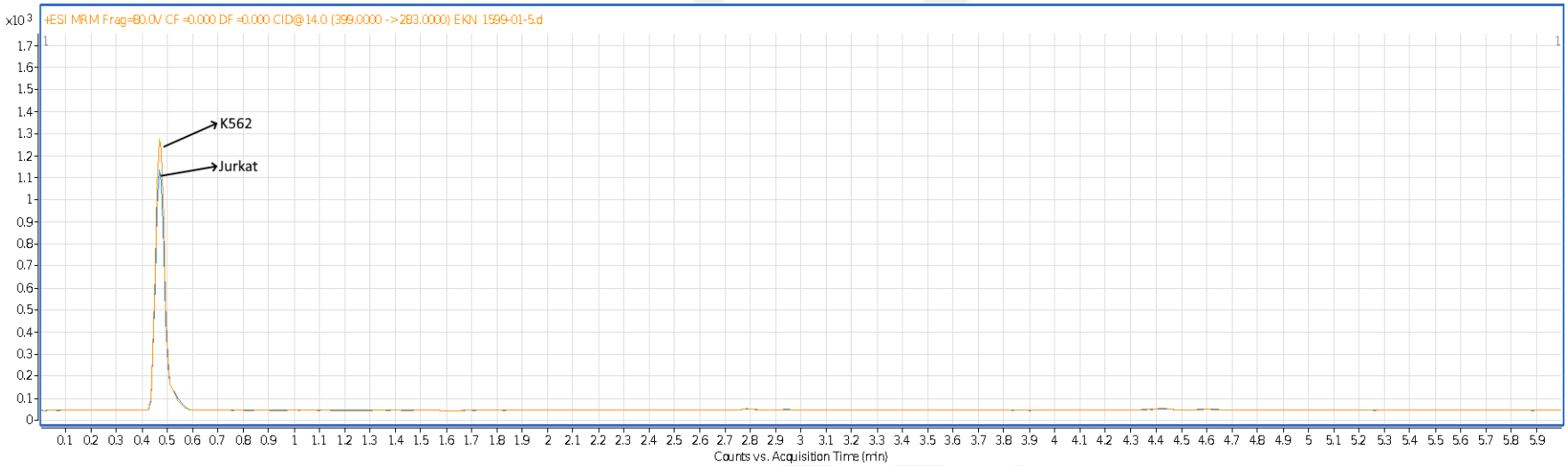

Figure 3.20: Comparative S-Adenosylmethionine Level in Cell Extracts. At this XIC, the orange peak shows K562 cell line and the blue peak shows the Jurkat cell line.

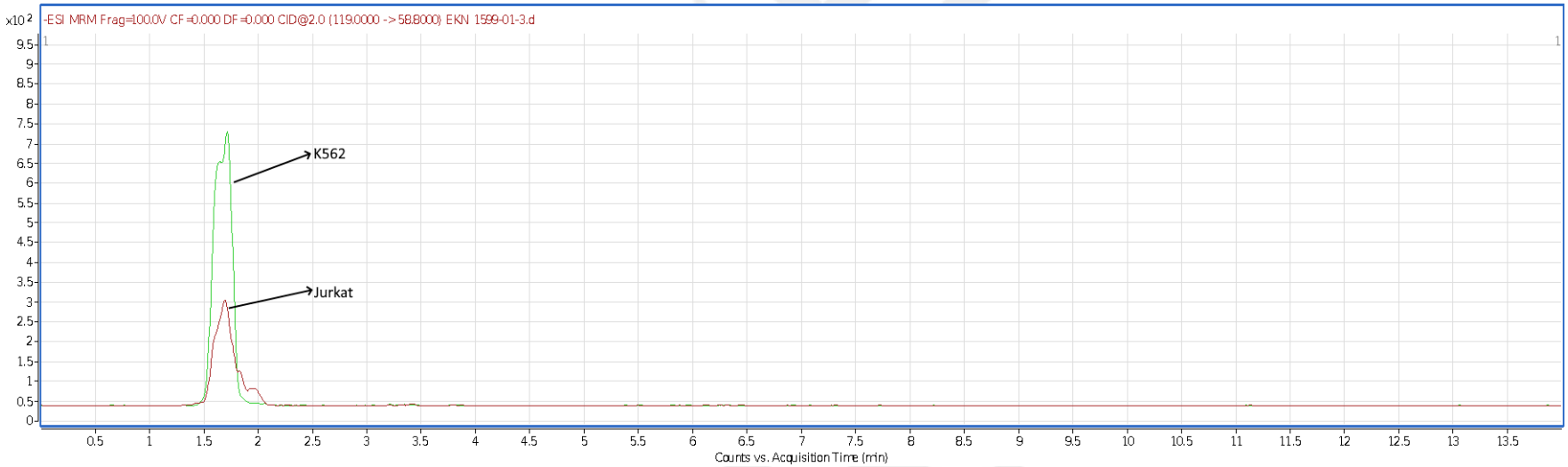

Figure 3.21: Comparative 3-Mercaptopyruvic acid Level in Cell Extracts. At this XIC, the green peak shows K562 cell line and the red peak shows the Jurkat cell line.

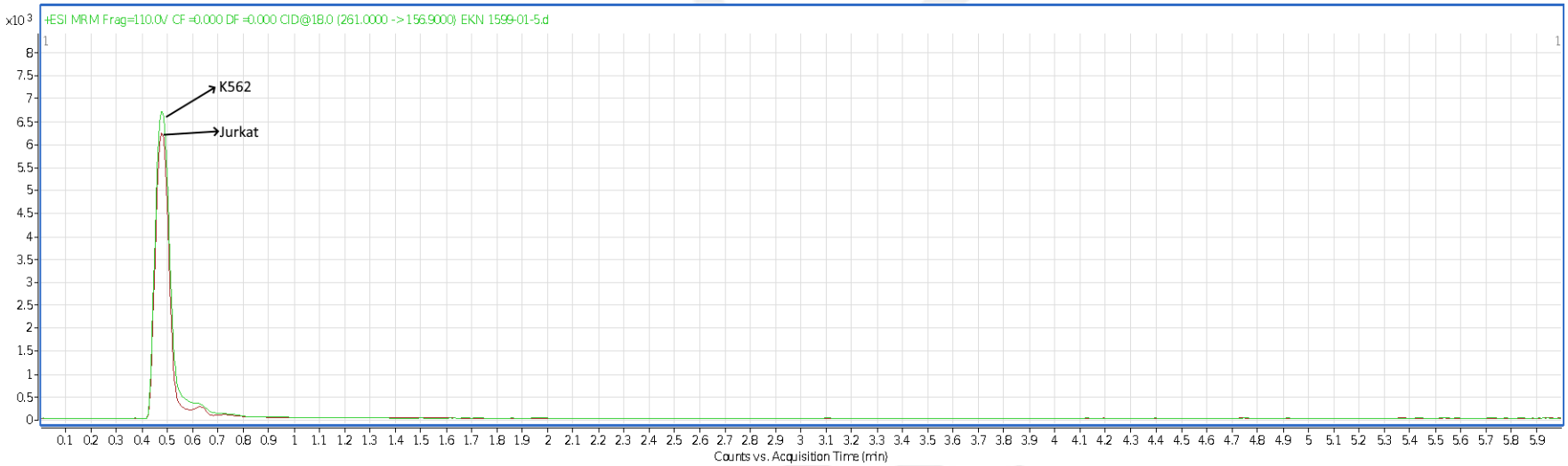

Figure 3.22: Comparative 5-Methylthioribose 1-phosphate Level in Cell Extracts. At this XIC, the green peak shows K562 cell line and the red peak shows the Jurkat cell line.

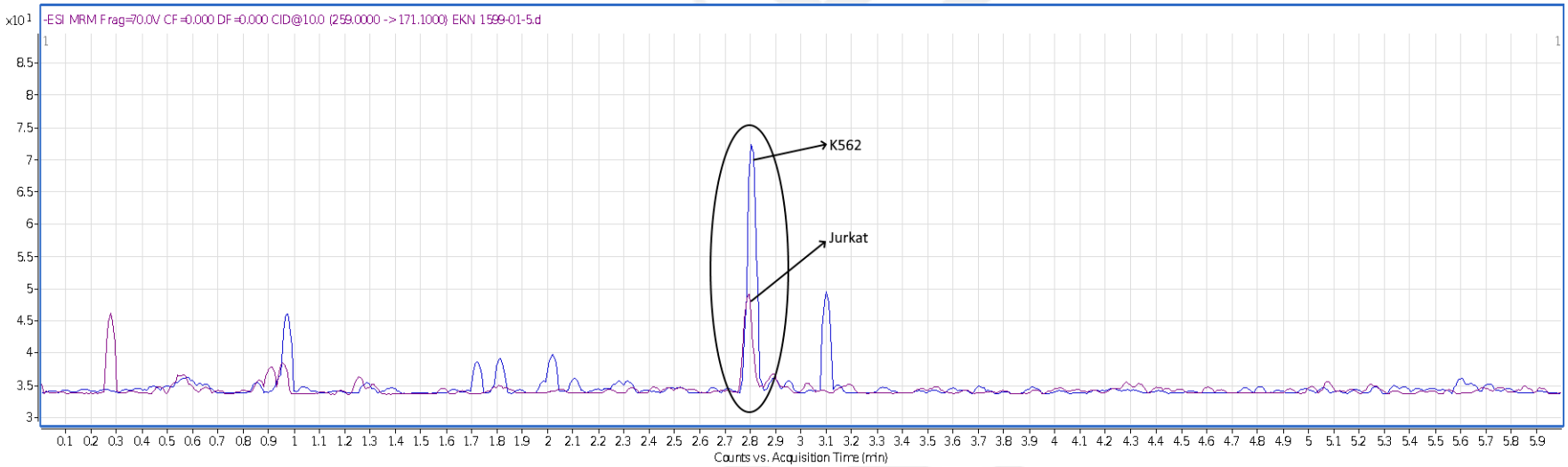

Figure 3.23: Comparative Glucose 1-phosphate Level in Cell Extracts. At this XIC, the blue peak shows K562 cell line and the purple peak shows the Jurkat cell line.

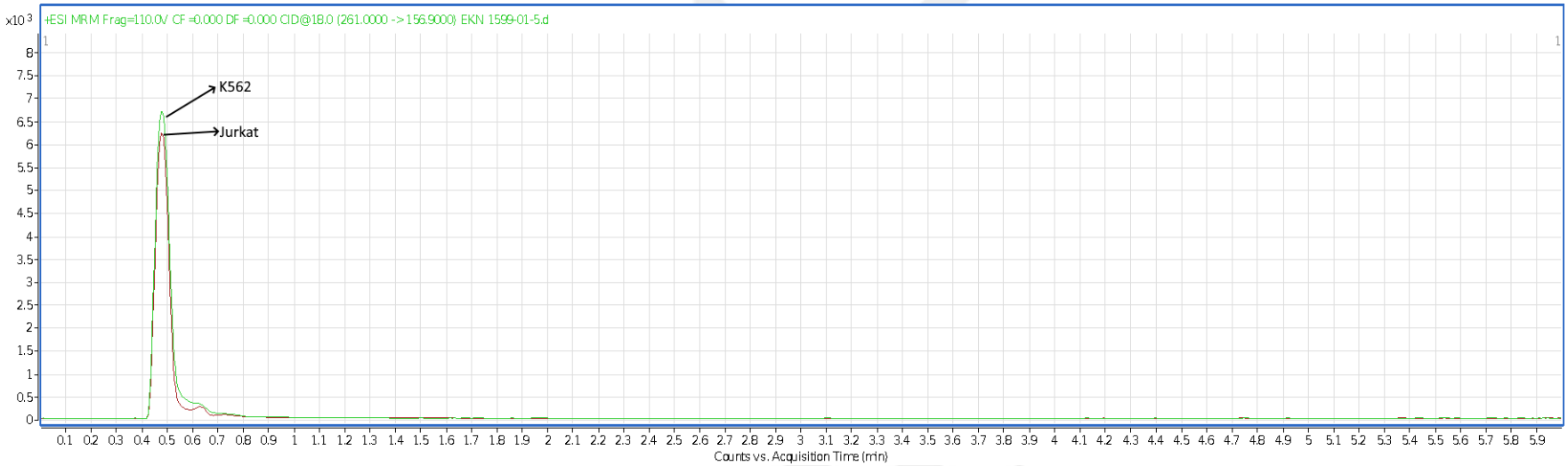

Figure 3.24: Comparative N-formyl L aspartate Level in Cell Extracts. At this XIC, the green peak shows K562 cell line and the red peak shows the Jurkat cell line.

In the table below, the fold changes of selected metabolites between cell lines were shown.

Table 3.12: Differential metabolites for discrimination between Jurkat and K562

m/z	KEGG ID	HMDB	Metabolites	Formula	Fold Change	Pathway
237.0	C01036	HMDB0002052	Maleylacetoacetic acid	C8H8O6	1	Tyrosine metabolism
237.0	C01061	HMDB0001268	4-Fumarylacetoacetic acid	C8H8O6	1	Tyrosine metabolism
175.1	C00062	HMDB0000517	L-Arginine	C6H14N4O2	2.1	Arginine and proline metabolism; Aminoacyl-tRNA biosynthesis; D-Arginine and D-ornithine metabolism
261.0	C00072	HMDB0000044	Ascorbic acid	C6H8O6	2.3	Glutathione metabolism; Ascorbate and aldarate metabolism
437.1	C00019	HMDB0001185	S-Adenosylmethionine	C15H23N6O5S	1.1	Cysteine and methionine metabolism; Arginine anda proline metabolism
179.0	C00957	HMDB0001368	3-Mercaptopyruvic acid	C3H4O3S	2.25	Cysteine and methionine metabolism
261.0	C04188	HMDB0000963	5-Methylthioribose 1-phosphate	C6H13O7PS	1	Cysteine and methionine metabolism
295.0	C00103	HMDB0001586	Glucose 1-phosphate	C6H13O9P	1.4	Glycolysis metabolism
198.0	C01044	HMDB0060495	N-formyl L aspartate	C5H7NO5	1.1	Histidine metabolism; Glyoxylate and dicarboxylate metabolism

CHAPTER 4

DISCUSSION

In many tumor cells, Lactate Dehydrogenase (LDH) is mutated and is not functional, thus produced lactate is not catalyzed back to pyruvate. From literature, we know that as the mutated LDH levels increase, the severity of the disease also increases. Since we know also that ALL is a more aggressive disease than CML, and during the acute transformation CML the disease becomes more severe and unpredictable. we selected lactic acid as one of our standards. Here we showed that lactic acid levels were 1,6 times higher in T-cell Acute Lymphoblastic Leukemia compared to Chronic Myeloid Leukemia. (Figure 3.1 and Figure 3.2)

Citric acid is known to be the most abundant TCA cycle metabolite in cells. In this study, we showed that citric acid levels were also 1,2 times higher in T-cell Acute Lymphoblastic Leukemia compared to Chronic Myeloid Leukemia. (Figure 3.3 and Figure 3.4)

And it is possible to say that there is an increased accumulation of both the metabolites in ALL compared to the CML.

After a throughout literature research, 3-Chlorotyrosine was selected as an indicator of AML. A meaningful ratio of the 3-Chlorotyrosine concentration among the cell lines was expected to be seen, but it was not detected.

Two methods were used during the study (Table 2.1). The "Quantification method", which was primarily used for the quantification of lactic acid and citric acid concentrations in Jurkat and K562 cells, was also used for mass screening of the cell lines, for optimization. Both of the methods gave similar results and clean peaks.

In literature, the main metabolisms that are upregulated or downregulated are stated, and by this informations, we can say that amino acid [52], glycolysis, and glutathionylation [51] metabolism are the common mainly manipulated metabolisms in CML and ALL. (Figure 4.1)

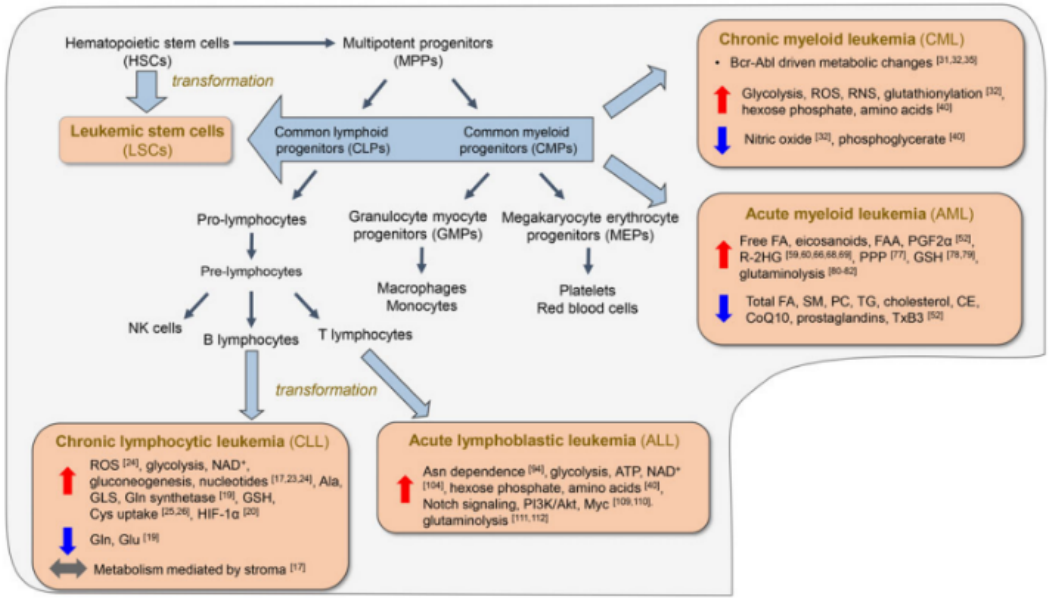

Figure 4.1: Upregulated and downregulated metabolisms in leukemia subtypes [53]

Consistent with the literature, we reported that metabolites that we detected in positive and negative mass screenings indicate that there are differences between the activities of main metabolomic pathways such as tyrosine, arginine and proline, and glutathione metabolisms in K562 and Jurkat cell lines. (Figure 3.15 and Figure 3.16)

Previous studies state that the reasons for the acute transformation of CML to ALL are not clearly known. It is known that if not treated, CML continues to evolve and reached the blast phase, and after this step, CML turns into AML, or interestingly, ALL by changing its origin to lymphoid cell line.

We showed that this conversion may be correlated to the metabolic changes in stated metabolic pathways.

After obtaining 127 estimated metabolites from the Peaks to Pathways program on MetaboAnalyst online platform, and down-scaling these to 42 with the help of the

Metabolite Set Enrichment Analysis and HMDB and KEGG databases, an literature study was conducted to select 9 metabolites which were studied in leukemia species (especially CML and ALL) the most, among these metabolites. The MS/MS analysis was then performed to confirm that the mass was indeed the determined metabolite.

Following a HMDB and KEGG scan to down-scale the number of metabolites to be focused on, we decided to work with maleylacetoacetic acid (or 4-fumaryl acetoacetic acid, since both give the same peaks at LC-MS and follow each other at the tyrosine metabolism), L-arginine, ascorbic acid, S-adenosylmethionine, 3-mercapto pyruvic acid, 5-methylthioribose-1-phosphate, glucose-1-phosphate, and N-formyl-L-aspartate (the precursor of L-asparagine, which is known to be used significantly higher in ALL cells).(Table 3.11)

After the LC-MS/MS analysis of the selected metabolites found in K562 and Jurkat cell lines, the peak areas of each analyte in both cell lines were used to obtain fold changes. The result shows that the concentrations of Maleylacetoacetic acid (or 4-Fumarylacetoacetic acid), 5-Methylthioribose 1-phosphate, and N-formyl L-aspartate are the same in K562 and Jurkat cell lines, whereas L-Arginine, Ascorbic acid and 3-Mercaptopyruvic acid is more than twice in concentration in K562 cell lines compared to Jurkat. S-Adenosylmethionine was not detected in the samples. (Table 3.12)

CHAPTER 5

CONCLUSIONS

In this study, we reported concentrations of lactic acid and citric acid metabolites to visualize the activity differences in the TCA cycle and lactate metabolism in Jurkat and K562 cell lines. We showed that citric acid and lactic acid levels were both higher in T-cell Acute Lymphoblastic Leukemia compared to Chronic Myeloid Leukemia in Blast Phase.

And with the quantification of lactic acid and citric acid, we were able to obtain fold changes and had an idea on the concentration of other selected metabolites.

Our study showed that there are differential activities in main pathways in CML and ALL cell lines, K562 and Jurkat, respectively.

REFERENCES

[1] N. C. Institute, "Chronic myelogenous leukemia treatment," *https://www.cancer.gov/types/leukemia/patient/cml-treatment-pdq*, Last visited at July 2019.

[2] R. Bott, "Leukemia, lymphoma, myeloma. toward a new understanding," *Igarss*, 2014.

[3] H. Okutan, "Lösemi nedir?," *http://www.losante.com.tr/Blog/Detail/2044*, Last visited at July 2019.

[4] H. Gralnick, A. Galton, D. Catovsky, C. Sultan, and J. M. Bennet, "Classification of acute leukemia.," *Annals of Internal Medicine*, 1977.

[5] C. Clarke and T. Holyoake, "Preclinical approaches in chronic myeloid leukemia: from cells to systems.," *Experimental Hematology*, 2017.

[6] "Kronik miyeloid lösemi," *http://www.thd.org.tr/THDHalk/?sayfakronikmiyeloid*, Last visited at May 2019.

[7] "Akut lenfoblastik lösemi," *http://www.thd.org.tr/THDHalk/?sayfa=akutlenfoblastik*, Last visited at July 2019.

[8]

[9]

[10]

[11]

[12]

[13] "Kronik lenfositer lösemi," *http://www.thd.org.tr/THDHalk/?sayfa=kroniklenfositer*, Last visited at May 2019.

[14] “Akut miyeloid lösemi,” *http://www.thd.org.tr/THDHalk/?sayfa=akutmiyeloid*, Last visited at May 2019.

[15] O. Fiehn, “Metabolomics–the link between genotypes and phenotypes.,” *Plant Molecular Biology*, 2002.

[16] B. Zhou, J. F. Xiao, L. Tuli, and H. W. Ressom, “Lc-ms-based metabolomics.,” *Mol Biosyst.*, 2012.

[17] J. Lindon and J. Nicholson, “Analytical technologies for metabonomics and 873 metabolomics, and multi-omic information recovery,” *Trac-Trend Anal Chem*, 2008.

[18] S. Becker, L. Kortz, C. Helmschrodt, J. Thiery, and U. Ceglarek, “Lc-ms-based metabolomics in the clinical laboratory,” *Journal of Chromatograhy B: Analytical Technolologies in Biomedical Life Sciences*, 2012.

[19] H. Gika, G. Theodoridis, R. Plumb, and I. Wilson, “Current practice of liquid chromatography-mass spectrometry in metabolomics and metabonomics,” *Journal of Pharmaceutical and Biomedical Analysis*, 2014.

[20] K. Spagou, H. Tsoukali, N. Raikos, H. Gika, I. Wilson, and G. Theodoridis, “Hydrophilic interaction chromatography coupled to ms for metabonomic/metabolomic studies,” *Journal of Separation Science*, 2010.

[21] I. Wilson, J. Nicholson, J. Castro-Perez, J. Granger, K. Johnson, B. Smith, and R. Plumb, “High resolution "ultra performance" liquid chromatography coupled to oa-tof mass spectrometry as a tool for differential metabolic pathway profiling in functional genomic studies,” *Journal of Proteome Research*, 2005.

[22] Q. Wu, H. Zhang, X. Dong, X. Chen, Z. Zhu, Z. Hong, and Y. Chai, “Uplc q-tof/ms based metabolomic profiling of serum and urine of hyperlipidemic rats induced by high fat diet,” *Journal of Pharmaceutical Analysis*, 2014.

[23] Agilent, “Basics of lc/ms,” *Agilent Website, Documents*, 1998.

[24]

[25] M. Hammarlund-Udenaes, E. C. de Lange, and R. G. Thorne, “Drug delivery to the brain: Physiological concepts, methodologies and approaches.,”

[26] K. V. Venkatesh, L. Darunte, and P. J. Bhat, "Warburg effect.," *Encyclopedia of Systems Biology.*, 2013.

[27] R. Karlíková, J. Široká, D. Friedecký, E. Faber, M. Hrdá, K. Mičová, I. Fikarová, A. Gardlo, H. Janečková, I. Vrobel, and T. Adam, "Metabolite profiling of the plasma and leukocytes of chronic myeloid leukemia patients.," *Journal of Proteome Research*, 2016.

[28] M. Calderón-Santiago, F. Priego-Capote, N. Turck, X. Robin, J. C. S. B Jurado-Gámez, and M. L. de Castro, "Human sweat metabolomics for lung cancer screening," *Anal. Bioanal. Chem*, 2015.

[29] S. J. Cameron, K. E. Lewis, M. Beckmann, G. G. Allison, R. Ghosal, P. Lewis, and L. Mur, "The metabolomic detection of lung cancer biomarkers in sputum," *Lung Cancer*, 2016.

[30] M. Gottschalk, G. Ivanova, D. M. Collins, A. Eustace, R. O'Connor, and D. F. Brougham, "Metabolomic studies of human lung carcinoma cell lines using in vitro 1h nmr of whole cells and cellular extracts," *NMR Biomed.*, 2008.

[31] I. Horváth, Z. Lázár, N. Gyulai, M. Kollai, and G. Losonczy, "Exhaled biomarkers in lung cancer," *Eur. Respir. J.*, 2009.

[32] Y. Li, X. Song, X. Zhao, L. Zou, and G. Xu, "Serum metabolic profiling study of lung cancer using ultra high performance liquid chromatography/quadrupole time of flight mass spectrometry," *J. Chromatogr. B Analyt. Technol. Biomed. Life Sci.*, 2014.

[33] S. Abbas, "Acquired mutations in the genes encoding idh1 and idh2 both are recurrent aberrations in acute myeloid leukemia: prevalence and prognostic value," *Blood*, 2010.

[34] H. Y. H, "Idh1 and idh2 mutations in gliomas," *New England Journal of Medicine*, 2009.

[35] M. F. Amary, "Idh1 and idh2 mutations are frequent events in central chondrosarcoma and central and periosteal chondromas but not in other mesenchymal tumours," *Journal of Pathology*, 2011.

[36] D. R. Borger, "Frequent mutation of isocitrate dehydrogenase (idh)1 and idh2 in cholangiocarcinoma identified through broad-based tumor genotyping," *Oncologist*, 2012.

[37] P. Paschka, "Idh1 and idh2 mutations are frequent genetic alterations in acute myeloid leukemia and confer adverse prognosis in cytogenetically normal acute myeloid leukemia with npm1 mutation without flt3 internal tandem duplication," *Journal of Clinical Oncology*, 2010.

[38] E. R. Mardis, "Recurring mutations found by sequencing an acute myeloid leukemia genome," *New England Journal of Medicine*, 2009.

[39] J. P. Bayley and P. Devilee, "Warburg tumours and the mechanisms of mitochondrial tumour suppressor genes. barking up the right tree?," *Current Opinion in Genetics and Development*, 2010.

[40] P. Gonçalves and F. Martel, "Butyrate and colorectal cancer: The role of butyrate transport," *Current Drug Metabolism*, 2013.

[41] E. Ackerstaff, B. R. Pflug, and a. Z. M. B. J B Nelson, "Detection of increased choline compounds with proton nuclear magnetic resonance spectroscopy subsequent to malignant transformation of human prostatic epithelial cells," *Cancer Research*, 2001.

[42] J. Tan and A. Le, "Breast cancer metabolism," *The Heterogeneity of Cancer Metabolism*, 2018.

[43] O. Warburg, F. Wind, and E. Negelein, "The metabolism of tumors in the body.," *J. Gen. Physiol.*, 1927.

[44] D. S. Wishart, R. Mandal, A. Stanislaus, and M. Ramirez-Gaona, "Cancer metabolomics and the human metabolome database.," *Metabolites*, 2016.

[45] W. Wojtowicz, A. Chachaj, A. Olczak, A. Ząbek, E. Piątkowska, J. Rybka, and P. Młynarz, "Serum nmr metabolomics to differentiate haematologic malignancies.," *Oncotarget*, 2018.

[46] M. Tiefenthaler, "Increased lactate production follows loss of mitochondrial

membrane potential during apoptosis of human leukaemia cells," *British Journal of Haematology*, 2001.

[47] S. Gottschalk, N. Anderson, C. Hainz, G. Eckhardt, and N. Serkova, "Imatinib (sti571)-mediated changes in glucose metabolism in human leukemia bcr-ablpositive cells," *Clinical Cancer Research*, 2004.

[48] S. Gross, R. A. Cairns, M. D. Minden, E. M, Driggers, M. A. Bittinger, H. G. Jang, M. Sasaki, S. Jin, D. P. Schenkein, S. M. Su, L. Dang, V. R, Fantin, and T. W. Mak, "Cancer-associated metabolite 2-hydroxyglutarate accumulates in acute myelogenous leukemia with isocitrate dehydrogenase 1 and 2 mutations," *The Journal of Experimental Medicine*, 2010.

[49] "Fda approves first targeted treatment for patients with relapsed or refractory acute myeloid leukemia who have a certain genetic mutation," *FDA NEWS RELEASE*, 2018.

[50] Y. Bai, H. Zhang, X. Sun, C. Sun, and L. Ren, "Biomarker identification and pathway analysis by serum metabolomics of childhood acute lymphoblastic leukemia.," *Clinica Chimica Acta*, 2014.

[51] R. Welner, G. Amabile, D. Bararia, and et al., "Treatment of chronic myelogenous leukemia by blocking cytokine alterations found in normal stem and progenitor cells," *Cancer Cell*, 2015.

[52] R. Karlikova, J. Siroka, D. Friedecky, and et al., "Metabolite profiling of the plasma and leukocytes of chronic myeloid leukemia patients," *Journal of Protein Research*, 2016.

[53] T. Nemkov, A. D'Alessandro, and J. A. Reisz, "Metabolic underpinnings of leukemia pathology and treatment," *Cancer Reports*, 2018.

[54] O. A. Kadhi, A. Melchini, R. Mithen, and S. Saha, "Development of a lc-ms/ms method for the simultaneous detection of tricarboxylic acid cycle intermediates in a range of biological matrices," *Journal of Analytical Methods in Chemistry*, 2017.

Appendix A

CALIBRATION CURVES FOR CITRIC ACID AND LACTIC ACID

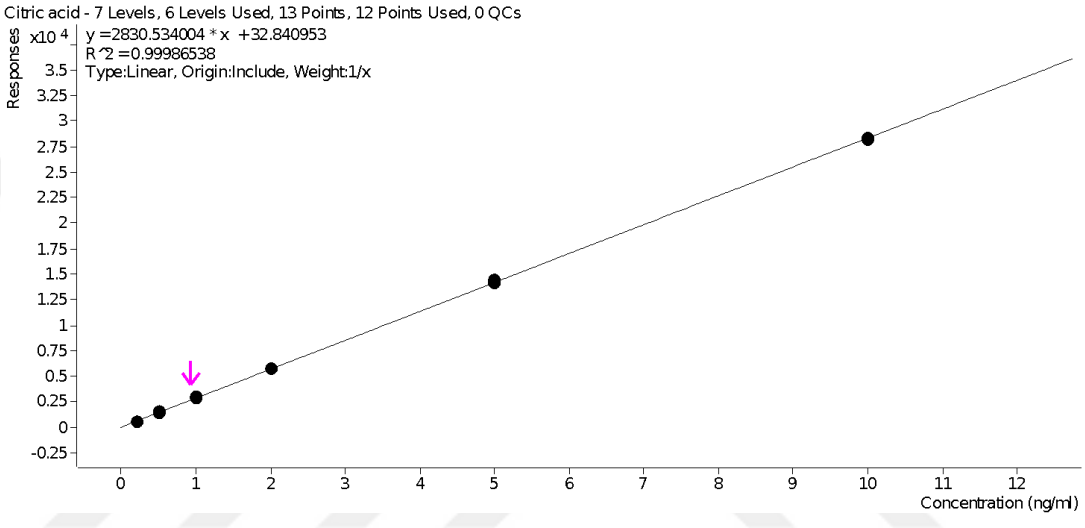

Figure A.1: Citric Curve. 0.2, 0.5, 1, 2, 5, 10 ppm

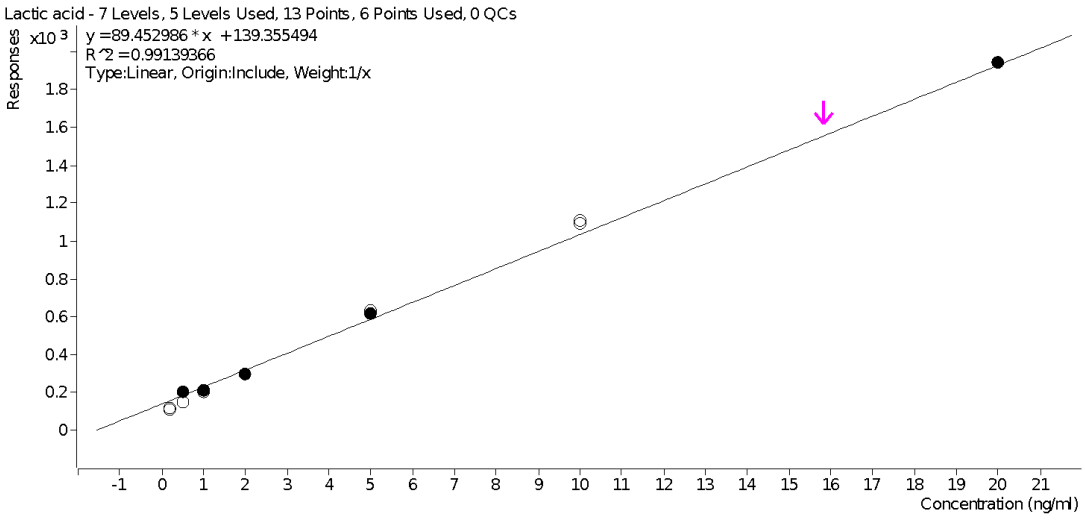

Figure A.2: Lactic Curve. 0.5, 1, 2, 5, 20 ppm

Appendix B

TABLE OF CRITICAL VALUES FOR TWO TAILED TEST

d.o.f.	0.05	0.01	0.001	d.o.f	0.05	0.01	0.001
1	12.706	63.657	636.619	23	2.069	2.807	3.768
2	4.303	9.925	31.599	24	2.064	2.797	3.745
3	3.182	5.841	12.924	25	2.06	2.787	3.725
4	2.776	4.604	8.61	26	2.056	2.779	3.707
5	2.571	4.032	6.869	27	2.052	2.771	3.69
6	2.447	3.707	5.959	28	2.048	2.763	3.674
7	2.365	3.499	5.408	29	2.045	2.756	3.659
8	2.306	3.355	5.041	30	2.042	2.75	3.646
9	2.262	3.25	4.781	40	2.021	2.704	3.551
10	2.228	3.169	4.587	50	2.009	2.678	3.496
11	2.201	3.106	4.437	60	2	2.66	3.46
12	2.179	3.055	4.318	70	1.994	2.648	3.435
13	2.16	3.012	4.221	80	1.99	2.639	3.416
14	2.145	2.977	4.14	90	1.987	2.632	3.402
15	2.131	2.947	4.073	100	1.984	2.626	3.391
16	2.12	2.921	4.015	120	1.98	2.617	3.373
17	2.11	2.898	3.965	150	1.976	2.609	3.357
18	2.101	2.878	3.922	200	1.972	2.601	3.34
19	2.093	2.861	3.883	300	1.968	2.592	3.323
20	2.086	2.845	3.85	500	1.965	2.586	3.31
21	2.08	2.831	3.819		1.96	2.576	3.291
22	2.074	2.819	3.792				